FREE VIBRATION ANALYSIS OF LAMINATED COMPOSITE SKEW PLATES WITH AND WITHOUT CUT-OUTS USING FINITE ELEMENT METHOD

Thesis Work in Partial Fulfillment of the Requirements for the

Award of the Degree of

Master of Engineering in Civil Engineering
(Specialization: *Structural Engineering*)

Submitted by

SOUMYENDRA NARAYAN ROY
EXAMINATION ROLL NO: M4CIV1601

ROLL NO.: 001010402004

Under the guidance of

Dr. SREYASHI DAS (nee PAL)

At the

Department of Civil Engineering
Faculty of Engineering & Technology
Jadavpur University
Kolkata-700032

CERTIFICATE OF RECOMMENDATION

This is to certify that the thesis titled, "FREE VIBRATION ANALYSIS OF LAMINATED COMPOSITE SKEW PLATES WITH AND WITHOUT CUT-OUTS USING FINITE ELEMENT METHOD", that is being submitted by Soumyendra Narayan Roy (Roll no. 001310402018 and exam Roll No. M4CIV1601) to Jadavpur University for the partial fulfillment of the requirements for awarding the degree of Master of Civil Engineering (Structural Engineering) is a record of bona fide research work carried out by him under my direct supervision & guidance.

The work contained in the thesis has not been submitted in part or full to any other university or institution or professional body for the award of any degree or diploma.

_____

Dr. SREYASHI DAS (nee PAL)
Assistant Professor
Department of Civil Engineering
Jadavpur University
Kolkata 700032

Countersigned by

_____
Prof. Ramendu Bikas Sahu

Head of the Department
Department of Civil Engineering
Jadavpur University
Kolkata 700032

_____
Prof. Shivaji Bandopadhyay

Dean, FET
Jadavpur University
Kolkata 700032

*CERTIFICATE OF APPROVAL**

This thesis paper **"FREE VIBRATION ANALYSIS OF LAMINATED COMPOSITE SKEW PLATES WITH AND WITHOUT CUT-OUTS USING FINITE ELEMENT METHOD"** submitted by Sri Soumyendra Narayan Roy (Exam. Roll no. M4CIV1601), is hereby approved as a credible study of an engineering subject carried out and presented in a manner satisfactory to warrant its acceptance as a prerequisite for the degree for which it has been submitted. It is understood that, by this approval the undersigned do not necessarily endorse or approve any statement made, opinion expressed or conclusion drawn therein but approved the thesis paper only for the purpose for which it is submitted.

Board of Thesis Paper Examiners:

1. _____

2. _____

*Only in case of the thesis is approved

ACKNOWLEDGEMENT

I would like to express my deep sense of gratitude to my respected teacher Prof. **Dr. SREYASHI DAS (nee PAL)**, Dept. of Civil Engineering, Jadavpur University, whose constant guidance and supervision encouraged me to carry out this thesis. She was a constant source of inspiration at all stages of my work. I am grateful to the Dean, Faculty of Engineering and Technology, Jadavpur University for giving me the opportunity to present this thesis. I am indebted to other faculty members of Civil Engineering Department for providing me encouragement at every stage of the work. I also wish to thank my friends for their kind assistance during the preparation of this thesis.

Date: _____

_____
SOUMYENDRA NARAYAN ROY
Roll No.:001310402018
Regn. No.:73917 of 1999-00
Exam Roll No.: M4CIV1601

Contents:

List of tables

List of figures

1 INTRODUCTION

1.1 General introduction

1.1.1 Composite laminates

A. General introduction to composites

Composite materials are not new in engineering applications. They have been used since antiquity. Wood and cob have been everyday composites. Israelites using bricks made of clay and reinforced with straw are an early example of application of composites. The individual constituents, clay and straw, could not serve the function by themselves but did when put together. In the Mongolian arcs, the compressed parts are made of corn, and the stretched parts are made of wood and cow tendons glued together. Ancient Pharaohs made their slaves use bricks with to straw to enhance the structural integrity of their buildings, some of which testify to wisdom of the dead civilization even today.

The needs of the high rise building and aerospace industry led to the development and application of modern advanced composite materials. Composite materials like laminates are being increasingly used in aerospace, civil, naval and other high performance engineering applications due to their light weight, high-specific strength and stiffness, excellent thermal characteristics, ease in fabrication and other significant attributes.

Advances in the manufacturing process and technology of laminated composites have changed the use of the composites from secondary structural components to the primary ones. Practically laminated composites are commonly used as a part of building like sandwich panel, aeronautical and aerospace industries as the main part of the structure rather than aluminum or other metallic materials. Advanced composite materials are widely used in defense, aircraft and space systems due to their advantages of high stiffness and strength-to-weight ratios. Low weight, high strength and greater rigidity are of paramount interest.

A composite is a structural material that consists of two or more combined constituents that are combined at a macroscopic level and are not soluble in each other. A reinforced concrete beam and a car tire are examples of such materials. The aim of this three-dimensional composition is to acquire a property which none of the constituents possesses. In other words, the target is to produce a material that possesses higher performance properties for a particular purpose than its constituent parts. Some of these properties are mechanical strength, corrosion resistance, high temperature resistance, heat conductibility, stiffness, lightness, and appearance.

In accordance with this definition, there are several conditions that must be satisfied by the composite material. It must be man-made and not natural. It must comprise at least two different materials with different chemical components separated by distinct interfaces. Different materials must be put together in a three-dimensional unity. It must possess properties which none of the constituents possesses alone and that must be the aim of its construction. A composite material usually derives its properties from its constituents. One constituent is called the reinforcing phase and the one in which it is embedded is called the matrix. The reinforcing phase material may be in the form of fibers, particles or flakes. The matrix phase materials are generally continuous.

B. Composition of composite materials

A composite material may be classified as fibrous, laminated and particulate. In fibrous composite materials, the fibers are embedded in the matrix. The load is mainly carried by the fibers. Fibrous composites consist of a large number of strong, stiff, continuous or chopped fibers embedded in a matrix having a large length to diameter ratio (100 or more) to ensure a reinforcing action. The matrix binds the fibers and distributes the load among the fibers and prevents the fibers from direct exposure to the environment. The fibers and the matrix may be of the same material or different materials. The fibers used in these material are characterized by their near crystal size diameter. In laminated composite materials, layers of different properties are bonded together to act as an integral part. In particulate composite materials, particles of different materials are held in a matrix.

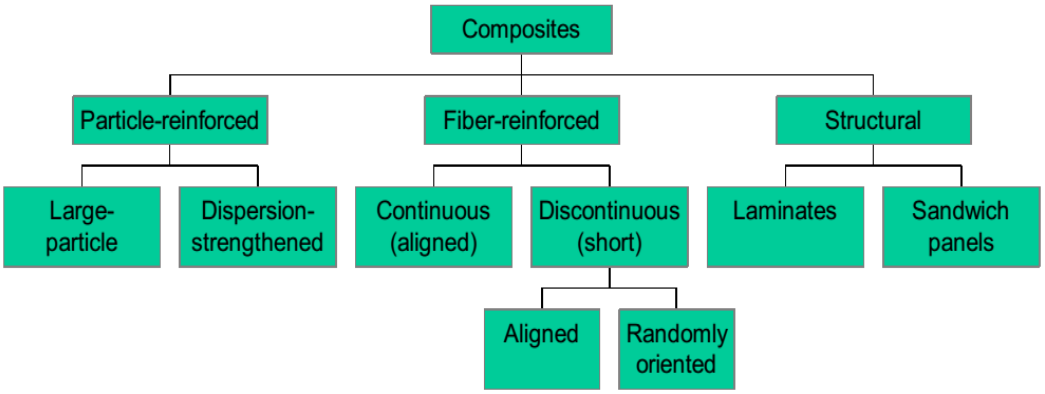

The properties of the composite material largely depend on the properties of the constituents, geometry and distribution of the phases. The distribution of the reinforcement determines the homogeneity or uniformity of the material system. The strength and stiffness of fibre reinforced composite materials increases in the fibre direction due to the continuity nature of fibre. Some more natural composites are available in the nature say wood, where the lignin matrix is reinforced with cellulose fibers and bones in which the bone-salt plates made of calcium and phosphate ions reinforce soft collagen. Composite systems include concrete reinforced with steel and epoxy reinforced with graphite/carbon/boron fibers etc.

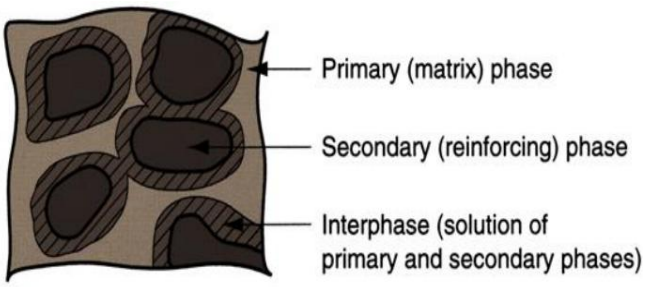

Figure 1.1 Schematic diagram of phases in a typical composite material

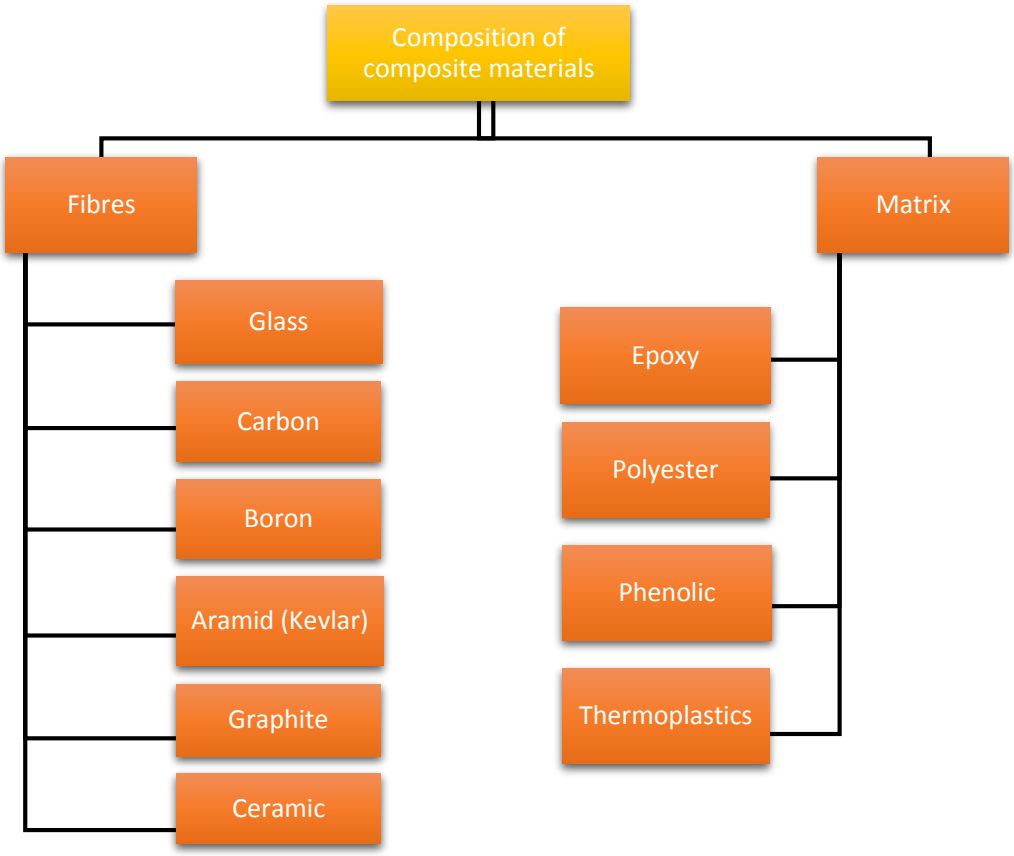

In matrix-based structural composites, the matrix serves two paramount purposes viz., binding the reinforcement phases in place and deforming to distribute the stresses among the constituent reinforcement materials under an applied force.

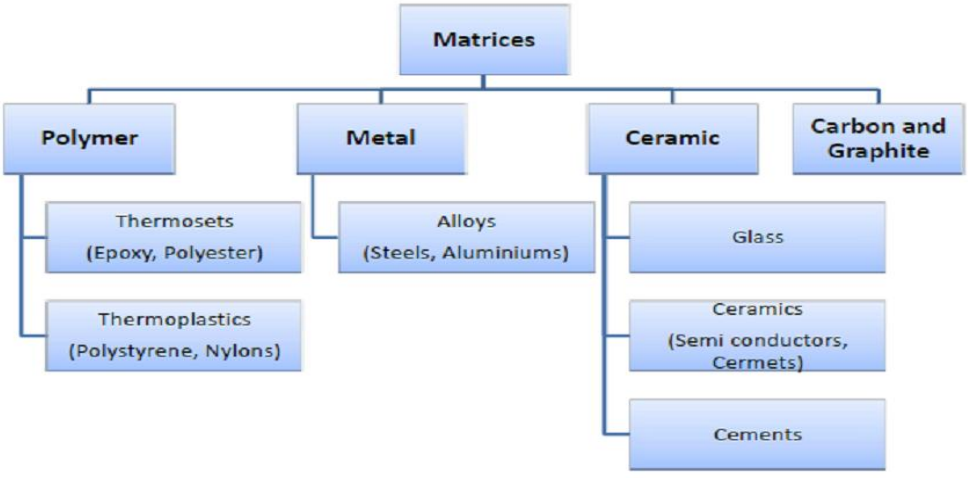

The demands on matrices are many. They may need to temperature variations, be conductors or resistors of electricity, have moisture sensitivity etc. This may offer weight advantages, ease of handling

and other merits which may also become applicable depending on the purpose for which matrices are chosen.

Solids that accommodate stress to incorporate other constituents provide strong bonds for the reinforcing phase are potential matrix materials. A few inorganic materials, polymers and metals have found applications as matrix materials in the designing of structural composites, with commendable success. These materials remain elastic till failure occurs and show decreased failure strain, when loaded in tension and compression

High performance thermoplastics are also being utilized on a large scale. It is generally considered that the reduction in weight up to 25% can be achieved by using fiber reinforced plastics in case of conventional materials of an aircraft. Glass-Epoxy composite materials were the first to be used in aircraft structures in mid-forties. Due to low specific stiffness of Glass-Epoxy, compared to conventional aircraft materials, it was not used in major applications. In around 1960 Graphite and Boron fibers were developed. Since, Graphite-Epoxy and Boron-Epoxy composite materials are superior to conventional metals used in aircrafts, in terms of both strength and stiffness, they were used in aircraft structural applications to a significant level. Graphite-Epoxy which is much cheaper than Boron-Epoxy, became very popular and has been used in aircraft structures, but to a smaller extent compared to Graphite-Epoxy composite materials.

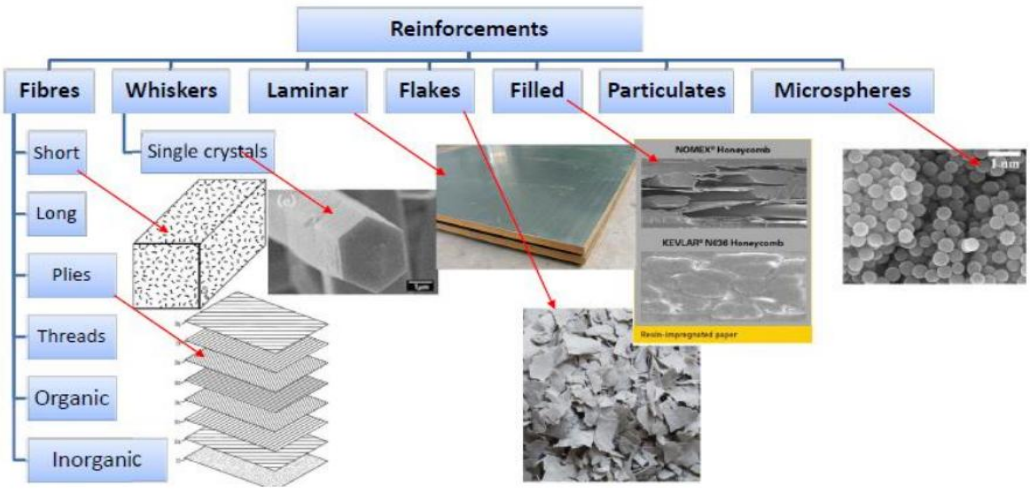

C. Laminated composites

Lamina is formed when an array of fibers is given a resin bath and hardened. The matrix transfers the loads to fibers. A number of laminae or plies are bonded together in different orientations to form a laminate. Laminae are homogeneous and anisotropic in macroscopic scale, and laminate is orthotropic. These are used in different structural forms such as beams, plates, shells, stiffened plates, stiffened shells etc. The low cost of assembly, ease of repair, high specific stiffness and strength, excellent damage tolerance and superior fatigue response characteristics increased the use of laminated composites in several important engineering fields.

A lamina, in general is a thin sheet with fibres oriented in some direction. Such a sheet can be characterized as two dimensional, with orthogonal material properties. It is, however, not capable of carrying any load. Hence, for practical purposes, a structure consisting of several laminae (laminate) is used.

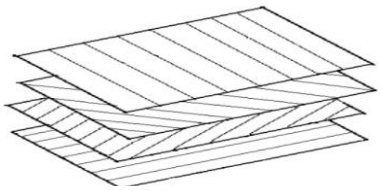

Figure 1.2 Laminate construction

In fiber reinforced plastic composites, first a thin lamina is prepared from fibers and matrix (sometimes a lamina may also be made of woven fabric). Laminae with different fiber orientations are bonded together to form an integral structural component, which is known as laminate. A lamina is considered to be homogeneous at macroscopic level. It has three planes of symmetry and hence termed as orthotropic. Its stress-strain behavior is usually treated as linear elastic. The laminates may be symmetric or anti-symmetric or unsymmetrical. They are also referred to as cross-ply or angle-ply depending on the fiber orientations of lamiae. If the fiber orientation in a lamina are 0^o or 90^o, it is called cross-ply and for any other fiber orientations, it is known as angle-ply.

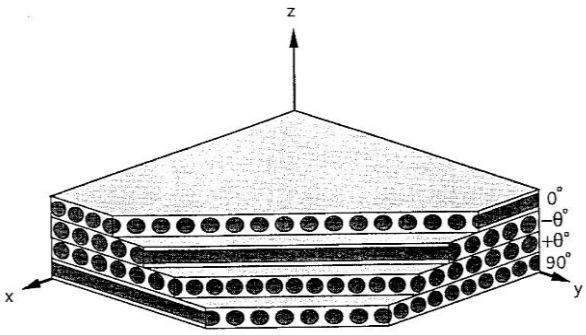

Figure 1.3 Laying scheme of a composite laminate

Figure 1.4 Composite laminate specimen

D. Classifications of composites

Depending on the matrix material, composites can be further classified into the following categories:

- Metal matrix composites (MMC)
- Polymer matrix composites (PMC)
- Ceramic matrix composites (CMC)

Depending on the reinforcement used, they can be classified into the following groups:

- Fibre reinforced composites
- Particle reinforced composites
- Flake/Plate reinforced composites

The laminates also classified based on the symmetricity of reinforced fibres, viz:

- Symmetric laminates
- Anti-symmetric laminates
- Non-symmetric laminates

E. Application of Composite Materials

Composites are one of the most widely used materials because of their adaptability to different situations and the relative ease of combination with other materials to serve specific purposes and exhibit desirable properties. Composite materials have wide application in various industries such as transportation, automobile, aerospace, marine, building, bio-engineering and so on. Some of the applications are described below.

Transportation: In surface transportation, reinforced plastics are the kind of composites used because of their huge size. They provide ample scope and receptiveness to design changes, materials and processes. The strength-weight ratio is higher than other materials. Their stiffness and cost effectiveness offered, apart from easy availability of raw materials, make them the obvious choice for applications in surface transportation. In heavy transport vehicles, the composites are used in processing of component parts with cost-effectiveness. Polyester resin with suitable fillers and reinforcements were the first applications of composites in road transportation. The choice was dictated by low cost, ease in designing and production of functional parts etc. permit both energy conservation and increased motoring economy. Reduction in the weight of an automobile structure achieves primary weight-saving and if carried to sufficiently great lengths enables the designer to use smaller power plants, thus achieving substantial secondary improvements in fuel economy. The majority of automotive applications involve glass-reinforced plastics because the extra cost of carbon or aramid fibre is rarely considered to be acceptable in this market. A wide range of car and truck body mouldings, panels and doors is currently in service, including complete front-end mouldings, fasciae, bumper mouldings, and various kinds of trim. There is considerable interest in the use of controlled crush components based on the high energy-absorbing qualities of materials like GRP. Selective reinforcement of aluminum alloy components, such as pistons and connecting rods, with alumina fibres is much discussed with reference to increased temperature capability.

Aerospace: A wide range of load-bearing and non-load-bearing components are already in use in both fixed-wing and rotary wing aircraft. Many military and civil aircraft now contain substantial quantities of lightweight, high-strength carbon, Kevlar and glass fibre composites, as laminated panels and mouldings and as composite honeycomb structures with metallic or resin-impregnated paper honeycomb core materials. They are used in air frames, wing spars, spoilers, tail-plane structures, fuel tanks, drop tanks, bulkheads, flooring, helicopter rotor blades, propellers, and structural components, pressured gas containers, radomes, nose and landing gear doors, fairings, engine nacelles (particularly where

containment capability is required for jet engines), air distribution ducts, seat components, access panels and so forth. Many modern light aircraft are being increasingly designed to contain as much lightweight composite material as possible. For elevated temperature applications carbon-fibre- reinforced carbon is in use. Concord's disk brakes use these materials, rocket nozzles and re-entry shields have been fashioned from it, and there are other possibilities for its use as static components in jet engines. Rocket motor casings and rocket launchers are also frequently made of reinforced plastics. Space applications offer many opportunities for employing light-weight, high-rigidity structures for structural purposes. Many of the requirements are the same as those for aeronautical structures, since there is a need to have low weight and high stiffness in order to minimize loads and avoid the occurrence of buckling frequencies. Dimensional stability is at a premium, for stable antennae and optical platforms, for example, and materials need to be transparent to radio-frequency waves and stable towards both UV radiation and moisture.

Automotive Engineering: Carbon-fibre-reinforced plastic and carbon components are in use for prosthetic purposes, such as in orthopedic fracture fixation plates, femoral stems for hip replacements, mandibular and maxillary prostheses (jaw remodeling, for example), and for external orthotic supports in cases of limb deformity etc. Pyrolytic carbon is used to manufacture heart valve components, and the substitution of a carbon/carbon composite is not unlikely. There have also been developments in the use of particulate hydroxyapatite as filler in a thermoplastic composite for bone remodeling or replacement.

Civil/Structural Engineering: Composites used in this field are mainly glass-reinforced plastics. The low inherent elastic modulus of GRP is easily overcome in buildings by the use of double curvature and folded-plate structures, thin GRP panels also offer the advantage of translucency. Glass-reinforced cement (GRC) products made with Cem-FIL (alkali-resistant glass fibres) are gradually being introduced as structural cement-based composites, but these GRC are still regarded with some suspicion by architects who prefer to consider only non-load-bearing applications for glass reinforced cement. Development of suitable highly-drawn polymer fibres and net-like polymeric reinforcement has made it possible to produce stable polymer-reinforced cement for a variety of purposes. A good deal of GRP is used in this industry for folded-plate structures, cladding panels, decorative ‘sculptured’ panels (like those in the doors of the Roman Catholic cathedral in Liverpool), services mouldings and ducting, racking, pipe work, rainwater mouldings, domestic and industrial water tanks, form-work for concrete, and complete small structures like foot-bridges. A vast range of pleasure craft has long been produced in GRP, but much serious use is also made of the same materials for hull and superstructure construction of passenger transport vessels, fishing boats and military (mine countermeasures) vessels. Sea-water cooling circuits may also be made of GRP as well as hulls and other structures. Off shore structures such as oil rigs also make use of reinforced plastics, especially if they can be shown to improve on the safety of steel structures, for fire protection piping circuits, walkways, flooring, ladders, tanks and storage vessels, blast panels, and accommodation modules. High specific compression properties also make composite materials attractive for submersibles and submarine structures, both for oil exploration and for military purposes, and for towed transducer arrays for sea- bed sonar mapping.

Sport Industry: Perhaps the most visible development in the use of composites has been in the sports goods industry. Manufacturers have been quick to seize on the potential advantages of new materials like carbon and boron fibre composites over conventional wood and metal for sports equipment of all kinds. GRP vaulting poles were perhaps the earliest of the composite sports gear, but one can now obtain tennis rackets, cricket bats, golf clubs, fishing rods, boats, oars, archery equipment, canoes and canoeing gear,

surf boards, wind-surfers, skateboards, skis, ski-poles, bicycles, and protective equipment of many sorts in composite materials of one kind or another. The main advantages of using composites are higher Specific Strength (strength-to weight ratio), design flexibility, corrosion resistance, durability, low relative investment etc.

Advanced composite materials are widely used in aircraft and space systems due to their advantages of high stiffness- and strength-to-weight ratios. However, the analysis of multi-layered structures is a complex task compared with conventional single layer metallic structures due to the exhibition of coupling among membrane, torsion and bending strains; weak transverse shear rigidities; and discontinuity of the mechanical characteristics along the thickness of the laminates. More accurate analytical/numerical analysis based on three-dimensional models may be computationally involved and expensive. Hence, among researchers, there is a growing appreciation of the importance of developing new kinematics for the evolution of accurate two dimensional theories for the analysis of thick laminates with high orthotropic ratio, leading to less expensive models. In this context, the applications of analytical/ numerical methods based on various higher-order theories, not only for the vibrations of thick laminates, but also for the high frequency vibrations of thin composite plates, has recently attracted the attention of several investigators/researchers. Increasing use of composite materials in the design of high-performance vehicles has attracted much attention to the dynamic behavior of structural components under service conditions. Experimental procedures can provide information on the real behavior of structures to the designer, but cannot cover all the design possibilities. Therefore, it is important to develop a general, as well as reliable, analysis procedure which can predict the response of composite laminates under a variety of service conditions. Considerable research effort has been devoted to the development of analytical procedures for the analysis of composite materials. This has resulted in a variety of laminated plate theories and solution methods including, among others, classical thin plate theory, first-order shear deformable theories and discrete laminate theories. Thin plate structures have wide usage area in aircraft, ships, vehicles and defense industry. Turbulences occurring in atmosphere, explosions, sonic booms, shock waves, etc. produce dynamic loads on the structures near them. Linear and nonlinear transient behavior of layered composite plates/shells under dynamic loads are among attractive research areas because of their increasing importance and multi parameter dependencies such as boundary conditions, fiber orientations, damping, plate thickness to span ratio, load duration, etc.

1.1.2 Cutouts

In general, plates are easily manufactured and are widely used for fabrication of structural members and eventually for the construction of marine and civil structures. Especially, a bolt-connection is a way of fastening plates by inserting bolts into the cutouts (or holes), which are made through designated areas of target plates that are to be connected. Making cutouts is not merely for connecting but also for reducing the weight of structural members.

The need for cutout in a subcomponent is typically required by practical concerns. For example, cutouts in wing spars and cover panels of commercial transport and military fighter aircraft wings are needed to provide access for hydraulic lines and for damage inspection. The designers often need to incorporate cutouts or openings in a structure to serve as doors and windows. These are also provided for access to and service of interior parts in aircrafts and in bridges having plated structures such as box girders. In liquid retaining structures cutouts at the bottom plate are needed for passage of liquid. Cutouts are required for ventilation as well. In some applications these structural elements having cutouts are

required primarily to resist buckling and in other cases they must carry load well into the post buckling stage in order to yield weight savings. Since the presence of cutouts generally reduce the strength, stiffness and inertia of the plate structure, so a detailed study needs to be done to evaluate their dynamic capacity.

1.1.3 Skew plates

It is observed from the existing literature that the large amplitude flexural vibration of rectangular and circular plates has received considerable attention of the researchers. However, limited work has been focused on the free vibration analysis of plates other than rectangular/circular plates. The plates with non-rectangular plan-forms like skew plates find wide application in the aerospace industry. Though a huge body of literature exists on the linear free vibration of isotropic and single layer orthotropic skew plates, such analysis concerning the laminated composite skew plates has received relatively little attention, despite the increasing use of such components in aircrafts.

It is well known that skew plates are often used in modern structures, despite the mathematical difficulties encountered in their analysis. Swept wings of airplanes, for example, can be idealized by introducing substructures in the form of oblique plates. Similarly, complex alignment problems in bridge designs are often solved by using skew plates. Numerous other applications of oblique parallelogram slabs can also be found in buildings. Skew plates and laminates are structural elements of practical importance in many engineering applications. To have an efficient and reliable design it is essential to employ an accurate analysis method to predict static, stability and dynamic behavior of such structural elements.

1.1.4 Finite element method

The Finite Element Method (FEM) is a numerical technique to find approximate solutions of partial differential equations. It was originated from the need of solving complex elasticity and structural analysis problems in Civil, Mechanical and Aerospace engineering. In a structural simulation, FEM helps in producing stiffness and strength visualizations. It also helps to minimize material weight and its cost of the structures. FEM allows for detailed visualization and indicates the distribution of stresses and strains inside the body of a structure. Many of FE software are powerful yet complex tool meant for professional engineers with the training and education necessary to properly interpret the results.

Several modern FEM packages include specific components such as fluid, thermal, electromagnetic and structural working environments. FEM allows entire designs to be constructed, refined and optimized before the design is manufactured. This powerful design tool has significantly improved both the standard of engineering designs and the methodology of the design process in many industrial applications. The use of FEM has significantly decreased the time to take products from concept to the production line. One must take the advantage of the advent of faster generation of personal computers for the analysis and design of engineering product with precision level of accuracy.

A. Concepts of Elements and Nodes

Any continuum/domain can be divided into a number of pieces with very small dimensions. These small pieces of finite dimension are called ‘Finite Elements’ (Fig. 1.5). A field quantity in each element is allowed to have a simple spatial variation which can be described by polynomial terms. Thus the original domain is considered as an assemblage of number of such small elements. These elements are connected through number of joints which are called ‘Nodes’. While discretizing the structural system, it is assumed

that the elements are attached to the adjacent elements only at the nodal points. Each element contains the material and geometrical properties. The material properties inside an element are assumed to be constant. The elements may be 1D elements, 2D elements or 3D elements. The physical object can be modeled by choosing appropriate element such as frame element, plate element, shell element, solid element, etc. All elements are then assembled to obtain the solution of the entire domain/structure under certain loading conditions. Nodes are assigned at a certain density throughout the continuum depending on the anticipated stress levels of a particular domain. Regions which will receive large amounts of stress variation usually have a higher node density than those which experience little or no stress.

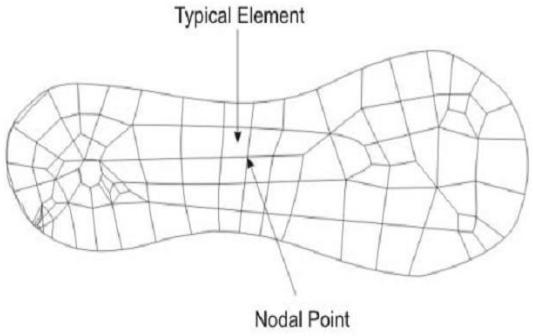

Figure 1.5 Finite element discretization of a domain

B. Idealization of a Continuum

A continuum may be discretized in different ways depending upon the geometrical configuration of the domain. Fig. 1.6 shows the various ways of idealizing a continuum based on the geometry.

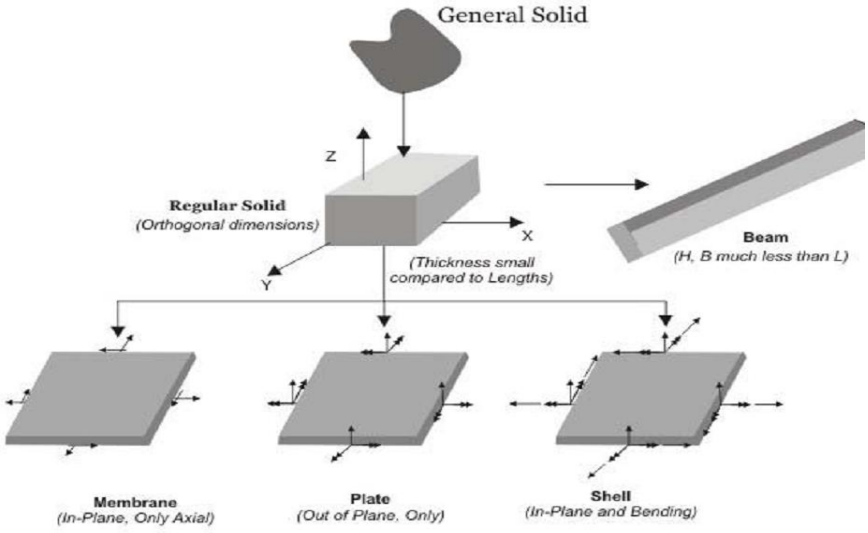

Fig. 1.6 Various ways of idealization of a Continuum

C. Discretisation Technique

The need of finite element analysis arises when the structural system in terms of its either geometry, material properties, boundary conditions or loadings is complex in nature. For such case, the whole

structure needs to be subdivided into smaller elements. The whole structure is then analyzed by the assemblage of all elements representing the complete structure including its all properties.

The subdivision process is an important task in finite element analysis and requires some skill and knowledge. In this procedure, first, the number, shape, size and configuration of elements have to be decided in such a manner that the real structure is simulated as closely as possible. The discretisation is to be in such that the results converge to the true solution. However, too fine mesh will lead to extra computational effort. Fig. 1.7 shows a finite element mesh of a continuum using triangular and quadrilateral elements. The assemblage of triangular elements in this case shows better representation of the continuum. The discretization process also shows that the more accurate representation is possible if the body is further subdivided into some finer mesh.

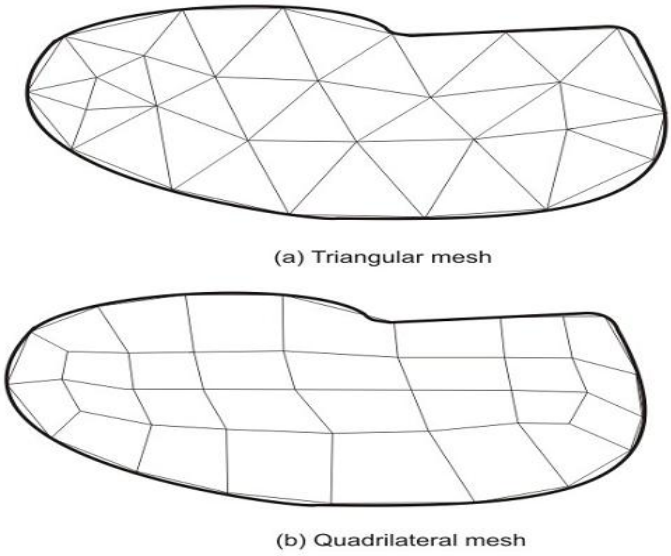

Figure 1.7 Discretisation of a continuum

D. Concepts of Finite Element Analysis

FEA consists of a computer model of a continuum that is stressed and analyzed for specific results. A continuum has infinite particles with continuous variation of material properties. Therefore, it needs to simplify to a finite size and is made up of an assemblage of substructures, components and members. Discretization process is necessary to convert whole structure to an assemblage of members/elements for determining its responses. Fig. 1.2.3 shows the process of idealization of actual structure to a finite element form to obtain the response results. The assumptions are required to be made by the experienced engineer with finite element background for getting appropriate response results. On the basis of assumptions, the appropriate constitutive model can be constructed.

For the linear-elastic-static analysis of structures, the final form of equation will be made in the form of $F=K_d$ where F, K and d are the nodal loads, global stiffness and nodal displacements respectively.

E. Advantages of FEA

1. The physical properties, which are intractable and complex for any closed bound solution, can be analyzed by this method.

2. It can take care of any geometry (may be regular or irregular).

3. It can take care of any boundary conditions.

4. Material anisotropy and non-homogeneity can be catered without much difficulty.

5. It can take care of any type of loading conditions.

6. This method is superior to other approximate methods like Galerkine and Rayleigh-Ritz methods.

7. In this method approximations are confined to small sub domains.

8. In this method, the admissible functions are valid over the simple domain and have nothing to do with boundary, however simple or complex it may be.

9. Enable to computer programming.

F. Disadvantages of FEA

1. Computational time involved in the solution of the problem is high.

2. For fluid dynamics problems some other methods of analysis may prove efficient than the FEM.

G. Errors and Accuracy in FEA

Every physical problem is formulated by simplifying certain assumptions. Solution to the problem, classical or numerical, is to be viewed within the constraints imposed by these simplifications. The material may be assumed to be homogeneous and isotropic; its behavior may be considered as linearly elastic; the prediction of the exact load in any type of structure is next to impossible. As such the true behavior of the structure is to be viewed with in these constraints and obvious errors creep in engineering calculations.

1. The results will be erroneous if any mistake occurs in the input data. As such, preparation of the input data should be made with great care.

2. When a continuum is discretised, an infinite degrees of freedom system is converted into a model having finite number of degrees of freedom. In a continuum, functions which are continuous are now replaced by ones which are piece-wise continuous within individual elements. Thus the actual continuum is represented by a set of approximations.

3. The accuracy depends to a great extent on the mesh grading of the continuum. In regions of high strain gradient, higher mesh grading is needed whereas in the regions of lower strain, the mesh chosen may be coarser. As the element size decreases, the discretisation error reduces.

4. Improper selection of shape of the element will lead to a considerable error in the solution. Triangle elements in the shape of an equilateral or rectangular element in the shape of a square will always perform better than those having unequal lengths of the sides. For very long shapes, the attainment of convergence is extremely slow.

5. In the finite element analysis, the boundary conditions are imposed at the nodes of the element whereas in an actual continuum, they are defined at the boundaries. Between the nodes, the actual boundary conditions will depend on the shape functions of the element forming the boundary.

6. Simplification of the boundary is another source of error. The domain may be reduced to the shape of polygon. If the mesh is refined, then the error involved in the discretized boundary may be reduced.

7. During arithmetic operations, the numbers would be constantly round-off to some fixed working length. These round–off errors may go on accumulating and then resulting accuracy of the solution may be greatly impaired.

1.1.5 Free and Forced Vibrations

Vibration is a mechanical phenomenon whereby oscillations occur about an equilibrium point. The oscillations may be periodic such as the motion of a pendulum or random such as the movement of a tire on a gravel road.

Free vibration: Free vibrations can be defined as oscillations about a system's equilibrium position that occur in the absence of an external excitation. It occurs when a mechanical system is set off with an initial input and then allowed to vibrate freely. It will vibrate in its natural frequency. If the system is undamped then it will vibrate forever but for damped systems the vibration will eventually die out. Examples of free vibrations are oscillations of a pendulum about a vertical equilibrium position and a motion of a vehicle suspension system after the vehicle encounters a pothole. Let's consider a mass attached to a spring, k and a damper, c (Figure 1.8). The mass is pulled to the right in horizontal direction and then released. Oscillations occur about its equilibrium position until it stops.

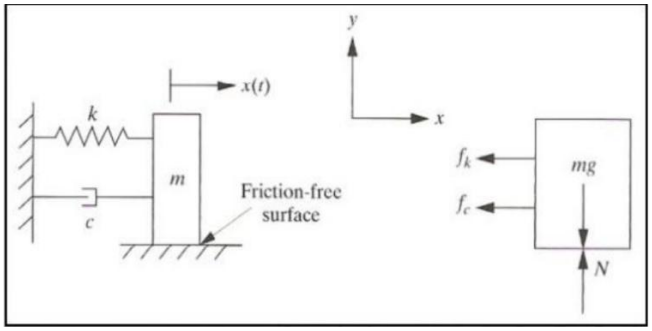

Figure 1.8 Free vibration- Free body Diagram

The governing equation for undamped and damped free vibration is shown below:

$$[M]\{\ddot{d}\} + [K]\{d\} = \{0\}$$

$$[M]\{\ddot{d}\} + [C]\{\dot{d}\} + [K]\{d\} = \{0\}$$

Forced vibration: Forced vibrations occur when work is being done on the system while the vibrations/oscillations occur. When an alternating force or motion is applied to a mechanical system then this phenomenon occurs. Examples of free vibrations include a motion caused by an unbalanced rotating component, a motion of reciprocating pistons in engine.

Diagram of forced vibration can be represented by a spring-mass-damper system with external force $F(t) = F_o \sin\omega t$ as shown in Fig. 1.9 Oscillations occur about its equilibrium position. Oscillations do not stop because of applied external force.

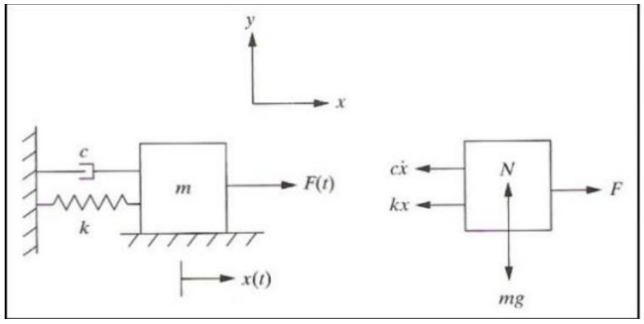

Figure 1.9 Forced vibration- Free body Diagram

The governing equation for undamped and damped forced vibration is shown below:

$$[M]\{\ddot{d}\} + [K]\{d\} = \{F\}$$

$$[M]\{\ddot{d}\} + [C]\{\dot{d}\} + [K]\{d\} = \{F\}$$

1.2 Objective of present study

Composite laminates with cutouts are extensively used in a diverse industrial field, especially, nuclear facilities, aeronautical, mechanical, marine, automotive and civil structures because of their many merits. Cutouts are useful for saving weight, for providing fuel, electrical and hydraulic lines. The plates having the cutouts reduce the total weight which in turn affect the vibration response similarly it also reduces the total stiffness and the bending behavior changes automatically.

Composite skew laminates with cutouts may result in a significant change of the dynamic characteristics around cutouts. Therefore, it is vital to study the effect of cutouts on the dynamic response of composite skew laminates. Skew members containing cutouts may result in more significant changes to their dynamic characteristics due to geometric change or mass loss. Generally, it is difficult to obtain exact solutions for the free vibration of skew laminates. Hence, one must make use of numerical methods to obtain approximate solutions.

The objective of the present study is to develop a finite element (FE) model of laminated composite skew plates with and without cutouts (centrally placed and square) and analyze the free vibration behavior.

1.3 Scope of present study

A computer program has been developed to study the influence of plate skewness as well as a centrally located square cutout on the dynamic properties of multilayered laminated composite plates. Nine-noded isoparametric plate elements with six degrees of freedom per node have been implemented in the present computations using FEM. First order transverse shear deformation based on Yang-Norris-Stavasky theory is used along with rotary inertia of the material. A three point gauss quadrature rule is applied for evaluating the bending stiffness matrix whereas, a two point gauss rule is applied for evaluating shear stiffness matrix to avoid shear locking. A set of results with various cut-out ratios and by varying and the thickness of plates, plate skew angle as well as he boundary conditions are presented.

A series of parametric case studies has been conducted on the laminated composite plates with cutout/skewness. Both external and internal parameters are varied to get a comprehensive idea about

the effect variation due to skew angle, boundary conditions, thickness and cut out ratio on the dynamic behavior of laminated composite plates. The following case studies are provided-

1. Effect of variation due to skew angle without cut out
2. Effect of variation due to boundary conditions
3. Effect of variation due to thickness
4. Effect of variation due to cut out ratio
5. Effect of variation due to skew angle for cut out ratio 0.4

ANSYS program is a comprehensive finite element package, which enables us to solve the nonlinear differential equation. ANSYS provides a rich graphics capability that can be used to display results of analysis on a high-resolution graphics output. The composite laminate was modeled in ANSYS (version 15) finite element package and solved using ANSYS (version 15) parametric design language (APDL) code. Effects of different elastic, geometric parameters, material properties, cutout geometries and skew angles on the vibration responses are obtained by using the developed FE model. The results are tabulated and presented along with the results of our computer generated code in the validation part of this thesis so that we also get an idea whether our results tally closely with those of ANSYS (version 15) or not.

These set of results can be used to understand the behaviour of composite plates under similar parametric conditions. Results of such comparative study can be used to reproduce results for plates having similar layup sequence.

2. LITERATURE REVIEW

2.1 Free Vibration of Laminated Composite Plate using Finite Element Method

The laminated plate theories are essential to provide accurate analysis of laminated composite plates and a variety of laminated plate theories have been developed in a large amount of literature. Liu and Li (1996) [1] presented a comparison of laminated theories based on displacement hypothesis. A selective review and survey of the theories with emphasis on estimation of transverse/interlaminar stresses in laminated composites was given by Kant and Swaminathan (2000) [2].

Generally the laminated plate theories are classified as follows:

1. Equivalent single layer (ESL) theories
2. Continuum-based 3D elasticity theory

The ESL theory can again be classified in four sub categories;

i. Classical lamination theory (CLT)

ii. The first-order shear deformation theory (FSDT) (referred to as Mindlin Plate theory in some literatures)

iii. Higher-order shear deformation theories (HSDT)

iv. Layer-wise lamination theory (LLT)

The earliest solution to the free vibration of composite plates was based on the Classical method which is based on Kirchhoff plate theory (1850)[3]. It is the simplest theory among others, but the shear deformation effects are neglected. It was found that the Kirchhoff (1850) [4] theory of plates under predicts deflections and over predicts natural frequencies. These so happens due to the neglect of transverse shear strains in the classical plate theory of Kirchhoff. Mindlin (1951) [5] introduced the concept of first order transverse shear deformation for isotropic plates to account for a more realistic analysis of moderately thick to thick plates. Herein, unlike Kirchhoff's proposition of normal to the middle plane before deformation remaining plane and normal to the middle surface after deformation, it was assumed that this normal remains plane but not necessarily normal to the middle plane after deformation. Mindlin's theory was first extended to laminated isotropic plates by Stavsky (1965) [6], and then to laminated anisotropic plates by Yang, Norris and Stavsky (YNS) (1966) [7], for better estimation of inter laminar shear stresses. This is an extension of Mindlin's two-dimensional theory [5] for flexural motions of isotropic elastic plates to arbitrarily laminated composite plates, including first - order shear deformation and rotary inertia effects, and popularly called the YNS theory. The first-order shear deformation theories (FSDT) provides a balance between computational efficiency and accuracy for the global structural behaviour of thin and moderately thick laminated composite plates.

Three-dimensional plate theories [8-12] can give more accurate results than lamination theories for complex three-dimensional stresses, but when the number of layers increases, the number of governing equations needed in these three-dimensional theories becomes large and the problem becomes intractable. Hence, lamination theories are commonly used in the dynamic analysis of composite plates

In the classical plate theory, the shear strains are assumed to be negligible. But, because the ratio of the in-plane Young's moduli E to the transverse shear moduli G is between 20 to 50 in modern composites and between 2.5 to 3.0 in isotropic materials [13], shear effects are significant for composite materials. As per Whitney and Srinivas experimental results show that (a) the classical plate theory under predicts the deflections and over predicts the natural frequencies because the transverse shear strains are neglected and (b) the effect of transverse shear deformations increases with increasing mode number. Also, the error grows with an increase in plate thickness. Hence, an adequate theory must account for an accurate distribution of transverse shear stresses.

Reissner [14-16] presented a stress-based shear-deformation plate theory in which the transverse shear stresses are determined by using the three-dimensional theory of elasticity. Basset [17] presented a displacement-based theory for shells in which he gave geometric constraints on the shape of the shear warping of the cross section by assuming that the displacement components can be expanded in series of powers of the thickness coordinate. Following the idea of Basset [17], Hildebrand, Reissner, and Thomas [18], Hencky [19], and Mindlin [5] presented the so-called first-order shear-deformation theory.

The free and forced vibration response of laminated composite plate structures was predicted by Srinivas et al.(1970)[21] using a nine-node Lagrangian plate-bending finite element with five engineering DOF per node that incorporated rotary inertia. It has been shown by Whitney (1969)[20]

and Srinivas (1970) [21] that first order shear deformable theory may be adequate to predict global behavior of laminated plates, e.g. lateral deflection or fundamental natural frequency, but it is not better than CPT in calculating in-plane stresses because it does not include the contributions of higher shear modes. Higher-order theories lead to improved estimates of in-plane stress distributions and of the flexural vibration characteristics. It was shown in Refs. [36-39] that higher-order shear-deformation theories provide accurate global estimates for the deflections, frequencies, and buckling loads for laminated plates and are efficient for problems not involving regions of acute discontinuities.

Since the boundary value problem of a structure constructed with composite laminates is extremely complex, approximate numerical techniques are often used to obtain the solution. The most popular tool has been the finite element method which is usually based on a variational formulation. Several different types of element geometries, interpolation schemes and formulation strategies have been introduced.

Mau et al. (1973)[23] studied the vibration analysis of laminated plates by a hybrid stress element. However, discontinuity of the transverse normal stress and assumption of constant transverse displacement through thickness were major shortcomings. Hinton (1976) [24, 25] considered the free vibration of cross-ply laminated plates using the finite strip and finite element methods. Bert and Chen (1978) [26] has employed the first-order shear deformation theory (FSDT) widely to establish finite element models for free vibration analysis of the composite laminated plates. The effects of lamination and extension–bending coupling, shear and twist curvature couplings on the lowest frequencies and corresponding mode shapes for free vibration of laminated anisotropic composite plates was investigated using a finite element method with quadratic interpolation functions and five engineering degrees of freedom (DOF). The free, transverse vibrations of thin isotropic plates of various shapes are investigated by Yoshihiro Narita (1979) [27] and analytical methods to deal with the free transverse vibration of thin elastic plates of various shapes and edge conditions is presented. The author introduces new series-type solutions which are mathematically exact, satisfying the differential equation of plate vibration. Reddy (1979) [28] used the quadratic isoparametric element to study the free vibration of anti-symmetric angle-ply laminated plates including the transverse shear deformation and rotary inertia.

However, the shear deformable laminate theory, whether it is the first or higher-order theory, has two critical deficiencies. The first is its lack of capability to describe local deformation precisely. Due to this, it is difficult to avoid error in calculating natural frequencies as well as in-plane stresses around laminar interfaces, especially, when shear rigidities of adjacent laminae are quite different (Sun 1973[22], Lo 1977[29]). The other deficiency is the violation of equilibrium of the plate because stress continuity at the interface is, in general, not satisfied. The need to eliminate these deficiencies has motivated the development of several discrete laminated plate theories (Srinivas 1973, Sun 1973, Seide 1980 [30]) in which variation of anisotropy in the laminate is properly incorporated. The discrete laminate theory not only removes the drawbacks of shear deformable theories noted above, but it also allows different boundary conditions to be specified in each layer. It may be regarded as the most general approach capable of accurately describing the mechanical behavior of any type of laminated plates. Use of discrete laminate theories appeared to give better in-plane stress distribution (Seide 1980) and more accurate natural frequencies (Sun 1975) However, this theory, in general, involves a large number of field equations, and consequently makes the problems quite complicated.

A basis often used for laminate theories is to assume a pattern of variation of displacements over the thickness of the plate. In such theories, which allow for shear deformation, the constitutive relations of transverse shear are, in general, not satisfied. As a result, it is not possible to avoid some error in evaluating the laminate stiffness. Since the effect of transverse shear deformation is significant in laminated composites, accuracy of analysis can be considerably affected. In particular, its effect becomes more critical in thick laminates or hybrid laminates made of layers with drastically different material properties. Many attempts have been made to treat the shear deformation realistically, but a standard procedure applicable to laminates of arbitrary construction is not available.

The vibration analysis of laminated plates was carried out by a mixed element based on refined laminated plate theory by Putcha and Reddy (1986) [31]. Owen and Lee presented a finite element vibration analysis of laminated plates based on refined theory. Craig and Dowe (1986) [32] considered the flexural vibration of symmetrically laminated composite rectangular plates using the finite strip method. R. S. Sandhu, W. E. Wolfe, S. J. Hong, and H. S. Chohan (1990) [33] presents a procedure based on a generalization of Reissner's method to incorporate the effect of transverse shear deformation in a consistent manner. A variational formulation of the consistent shear deformable discrete laminate theory of laminated composite plates is also proposed. Various theories of homogeneous laminated plates are extended to study the buckling and free vibration behavior of nonhomogeneous rectangular composite laminates in the paper by Fares and Zenkour (1999) [34]. A strip element method for the transient analysis of symmetric laminated plates was presented by Y.Y. Wang, K.Y. Lam and G.R. Liu (2001) [35] to investigate the transient response of symmetric laminated plates. In this method, the two-dimensional governing equations based on the classical laminated plate theory is reduced to a set of ordinary differential equations using the principle of minimum potential energy.

2.2 Free Vibration of Laminated Composite Plates with cut-outs

References dealing with free vibration response of composite plates with cutouts are relatively less in number. Paramasivam (1973) [40] proposed a method to determine the effect of square openings on the fundamental frequency of square isotropic plates for different boundary conditions using the finite difference method. Results were obtained for simply supported and clamped boundary conditions. Aksu and Ali (1976) [41] developed a theory to study the dynamic characteristics of isotropic and orthotropic rectangular plates with one or two rectangular cutouts. They employed a method based on the use of variational principles in conjunction with finite difference technique. Rajamani and Prabhakaran (1977) [42, 43] studied the effect of a centrally located square cutout on the natural frequencies of square, simply supported and clamped symmetrically laminated composite plates for free and forced vibration cases. They assumed that the effect of cutout is equivalent to an external loading. Some of the conclusions drawn were: cutouts make plates less stiff for medium cutout sizes for all modulus ratios; the fundamental frequency increases with the increase in fiber orientation for all cutout parameters and for all modulus ratios; higher modes interchange for all modulus ratios except in few cases; the fundamental frequency increases with the cutout ratio for the 45^{o} fiber orientation only for all modulus ratios. Ali and Atwal (1980) [44] presented a simplified method, based on Rayleigh's principle, for the dynamic analysis of plates with rectangular cutouts. Results were obtained for a simply supported square plate with square and rectangular openings of selected size. Reddy (1982) [45] studied large amplitude flexural vibrations of rectangular plates, using a finite element formulation based on the Reissner–Mindlin theory in conjunction with non-linear (large rotation) strain displacement relations.

Numerical results dealing with the effect of parameters like side-to-thickness ratio, plate side-to-cutout side ratio and anisotropy were presented for both linear as well as non-linear frequencies. It was shown that the effect of shear deformation is more pronounced in the case of clamped plates than in simply supported plates. The effect of transverse shear was found to be more pronounced on higher modes than on fundamental mode. Lee et al.(1987) [46] presented a numerical method based on the Rayleigh principle and using CLPT for obtaining natural frequencies of a simply supported composite rectangular plate having a central rectangular cutout and double square cutouts. Chang and Chiang (1988) [47] used Hamilton's variational principle, the Mindlin plate theory and finite element method to study the effect of boundary conditions on a few selected natural frequencies of an isotropic plate having a square cutout on few selected natural frequencies. They used an eight noded quadratic element and compared results with those of Nagaya (1981) [48, 49]. Mundkar et al. (1994) [50] studied vibration of square isotropic plates with square cutouts assuming boundary characteristic orthogonal polynomial functions. Trends of first six frequencies were discussed for five types of boundary conditions. Sabir and Davies (1997) [51] used finite element method to determine natural frequencies of flat square plates containing an eccentrically located square hole. Plates were subjected to in-plane uniaxial or biaxial compression or uniformly distributed shear along the four outer edges, which were either simply supported or clamped. Rossi (1999) [52] used a standard code, based on finite element method, to study the effect of support constraints on inner and outer edges of a rectangular cutout and the cutout ratio on the fundamental frequency of thin, orthotropic rectangular plates. Aspect ratios of both the plate and the cutout were kept same. It was concluded that the fundamental frequency increases with increasing aspect ratio, increasing cutout ratio and with increasing constraints at boundaries. Chen et al. (2000) [53] investigated the free vibration response of symmetrically laminated, thick, doubly connected plates of arbitrary plate perimeter for the outer boundary and a hole defined by a super-elliptical equation capable to describe a rectangular and an ellipse. They used Rayleigh–Ritz method in conjunction with Reddy's higher order theory. The effect of laminate lay-up, length-to-thickness ratio, aspect ratio, stacking angle, cutout geometry, and boundary conditions on natural frequencies was examined. Kumar A, Shrivastava RP (2005) [54] developed a finite element formulation based on Higher Order Shear Deformation Theory to study the free vibration response of thick square composite plates having a central rectangular cutout, with and without the presence of a delamination around the cutout. An attempt was made to gain a complete understanding of the effect of a rectangular cutout on natural frequencies of the laminate. The concept of a frequency envelope was found to be quite convenient for this purpose. A systematic study was carried out to investigate the effect of material orthotropy, boundary conditions and side to-thickness ratio on the free vibration response. In addition, effects of delamination size and its location around the cutout on the natural frequency of a thick square laminate were examined. A comparison was also made between results obtained using First Order Shear Deformation Theory and Higher Order Shear Deformation Theory. Hota and Padhi (2007) [55] carried out amalgamation of a subparametric triangular plate bending element with first-order shear deformation and an approach that maintains uniform mesh sizes and shapes even while dealing with cutouts of arbitrary shapes. This was a distinct improvement over the existing practices of cutout modeling. Further the formulation being based on the subparametric element had the advantage of achieving matching modes, which enabled the model to deal problems of very thin plates without even going for reduced integration. Numerical examples on free vibration of plates with cutouts was analysed and the results presented together with those available in published literature. Dash, Asha and Sahu (2004) [56] carried out vibration and stability of laminated composite curved panels with cutouts using finite element method. The first order shear deformation (FSDT) was

used to model the curved panels, considering the effects of transverse shear deformation and rotary inertia. Since the stress field was non-uniform due to cutout, plane stress analysis is carried out using the finite element method to determine the stresses and these are used to formulate the geometric stiffness matrix. The Global Matrices are obtained using skyline techniques. The eigenvalues were obtained using subspace iteration scheme. The study revealed that the fundamental frequencies of vibration of an angle ply flat panel decrease with introduction of small cutouts but again rise with increase in size of cutout. However the higher frequencies of vibration continue to decrease up to a moderate size of cutout and then rise with further increase of size of cutout. The frequencies of vibration increase with introduction of curvature in the flat panel with cutout. However, the effect of curvature is reduced with increase of size of cutout. Sivakumar, Iyengar and Deb (1999) [57] carried out free vibration analysis of composite plates in the presence of cutouts undergoing large amplitude oscillations. The Ritz finite element model using a nine noded C^o continuity, isoparametric quadrilateral element along with a higher order displacement theory which accounts for parabolic variation of transverse shear stresses was used to predict the dynamic behavior. Results were obtained for laminated plates with various cutout geometries such as square, rectangle, circle and ellipse in the large amplitude range. Backbone curves were drawn for various boundary conditions and aspect ratios of thecutout. Iyengar and Bhavani Prasad (2010) [58] investigated the optimal designs of freely vibrating composite laminates with and without cutout. A simple higher order shear deformation theory (HSDT) with four unknown displacements was employed to obtain the vibration response. A C^1 continuity shear flexible element based on HSDT using the Hermite cubic polynomial is used for the rectangular element. The optimisation exercise was performed using genetic algorithms to maximize the fundamental frequency of vibration. The aspect ratio of the laminate, fibre orientation, thickness of plies, modulus are treated as design variables. On the basis of the investigation, it was observed that the non-dimensional frequency of the laminate with cutout can be higher or lower than those of the laminate without cutout depending on the size of the cutout. The presence of cutout significantly affects the frequency. Laura, Verniere De Irassar and Ercoli (1981) [59] obtained an approximate solution of fundamental frequency of a rectangular plate with a free, straight corner cutout by using the Ritz method. It was assumed that the edges of the rectangular plate are elastically retrained against rotation and that translation is prevented. The displacement amplitude was approximated in terms of a polynomial coordinate function which identically satisfied the prescribed boundary conditions along the orthogonal edges but not along the corner cutout. The analytical predictions were in reasonably good agreement with experimental results performed on a rigidly clamped square plate. Turvey, Mulcahy and Widden [60] carried out experiments to determine the free vibration frequencies and mode shapes of 3.2 mm thick, square plates with six combinations of clamped (C), simply supported (S) and free (F) edge supports. Comparison of experimental and theoretical/numerical frequencies confirmed that thin homogeneous orthotropic/anisotropic plate theory provides a reasonable model for predicting the free vibration response of plates. Additional vibration experiments were carried out on plates with central circular cutouts. The hole size ratios were varied from about 0.1 to 0.4 for three combinations of clamped (C) and simply supported (S) edge conditions. Finite element (FE) frequency and mode shape predictions based on orthotropic plate theory were again shown to be in reasonable agreement with the experimental frequencies and modes. Khdeir and Reddy [61] obtained a complete set of linear equations of the second-order theory of laminated composite plates. A generalized Levy type solution in conjunction with the state space concept was used to analyze the free vibration behavior of cross-ply and antisymmetric angle-ply laminated plates. Exact fundamental frequencies of cross-ply plate strips were obtained from arbitrary boundary conditions. The exact analytical solutions were obtained for thick and moderately thick plates

as well as for thin plates and plate strips. It was shown that the results of the second-order theory were very close to the results of the first-order and third-order theories reported in the literature, and different from those of the classical Kirchhoff's theory for thick laminates. Lee, Lim and Chow [62] presented a simple numerical method based on the Rayleigh principle for predicting the natural frequencies of composite rectangular plates which exhibit special and general orthotropy. The method was illustrated for simply-supported rectangular plates having central rectangular cutouts and double square cutouts. The results were compared with the reported finite element and analytical results. Some semi-analytical approaches for dealing problems on cutouts of shapes other than rectangular and of arbitrary ones exists [63, 64, 65]. Reddy (1984) [66] studied the effect of square cutout on the behavior of the laminated plate undergoing large amplitude vibration.

2.3 Free Vibration of Skew Laminated Composite Plates with cut-outs

Even less literature is available for analysis of skew laminated plates. A. Houmat (2015) [67] presented results for variable stiffness symmetric skew laminates with different fiber configurations showing
the effects of variation in skew angle on frequency and degree of hardening. The governing equations are based on thin plate theory and Von Karman strains. Nonlinear free vibration analysis of thin-to-moderately thick laminated composite skew plates was presented by P. Malekzadeh (2008) [68] based on the first order shear deformation theory (FSDT) using differential quadrature method (DQM). The geometrical nonlinearity is modeled using Green' strain and von Karman assumptions in conjunction with the FSDT of plates. The effects of skew angle, thickness-to-length ratio, aspect ratio and also the impact due to differenttypes of boundary conditions on the convergence and accuracy of the method are studied.Large amplitude free flexural vibration behavior of symmetrically laminated composite skew plates was investigated by M.K. Singha and Rupesh Daripa ((2007)) [69] using the finite element method. The formulation includes the effects of shear deformation, in-plane and rotary inertia. The variation of nonlinear frequency ratios with amplitudes was brought out considering different parameters such as skew angle, fiber orientation and boundary condition. The large amplitude free flexural vibration behaviors of thin laminated composite skew plates are investigated using finite element approach by Maloy K. Singha and M. Ganapathi (2004) [70] also. The variation of non-linear frequency ratios with amplitudes is brought out considering different parameters such as skew angle, number of layers, fiber orientation, boundary condition and aspect ratio. The influence of higher vibration modes on the non-linear dynamic behavior of laminated skew plates is also highlighted. Here it was found that the degree of hardening behavior increases with the skew angle and its rate of change depends on the level of amplitude of vibration. S. Wang (1997) [71] presented a B-spline Rayleigh-Ritz method (RRM) for free vibration analysis of skew fibre-reinforced composite laminates which may have arbitrary lay-ups, admitting the possibility of coupling between in-plane and out-of-plane behaviour and general anisotropy. This method is shown to be accurate and efficient.

Literature available for analysis of skew laminated plates with holes/ cut-outs is very rare indeed. Sang-Youl Lee (2010) [72] carried out the finite element dynamic stability analysis of laminated composite skew structures subjected to in-plane pulsating forces based on the higher-order shear deformation theory (HSDT). The two boundaries of the instability regions were determined using the method proposed by Bolotin. For laminated skew plate structures containing cutout, the effect of the interactions between the skew angle and other various parameters, for example, cutout size, the fiber angle of layer and thickness-to-length ratio were shown. T. Park, S.Y. Lee and G.Z. Voyiadjis (2009) [73] carried out free

vibration analysis of laminated composite skew plates with delamination around a centrally located quadrilateral cutout based on the high-order shear deformation theory (HSDT). In the finite element formulation for the delamination around cutout, the seven degrees-of freedom per node are used. The results for skew plates in this study mainly show the effect of the interactions between the skew angle and other various parameters, for example, cutout size, delamination area, and length-to-thickness ratio.

3. THEORY

3.1 Governing Dynamic Equations

Unlike the case of a rigid body, only Newton's second law of motion is not sufficient to derive the laws of motion for a deformable continuum. Here, the governing equation for an elastic body, subjected to time-dependent loading, is derived from the d'Alembert's principle, which is an alternative way to express the Newton's second law of motion, written as follows:

$$\vec{F} - m\vec{a} = 0 \tag{1}$$

where, the vector $-m\vec{a}$ is considered to be an inertial pseudo-force, $\vec{F}$ is the force acting on the mass m, while a is the acceleration of the mass, with the result that the above equation assumes a look similar to the equation of statics. For a deformable continuum, the inertia force is $-\int \rho \partial^2 \vec{u}/\partial t^2 \, dV$ and is a distributed body force by nature. Here ρ, $\vec{u}$, V and t signifies mass density, displacement of the mass, volume and time variable, respectively. The following relation, derived from the principle of virtual displacement

$$\iiint_V B_i \delta u_i dV + \oiint_S T_i^{(n)} \delta u_i dS - \iiint_V \sigma_{ij} \delta \varepsilon_{ij} dV = 0, \tag{2}$$

is also a valid equation of static equilibrium and may be generalised to include the dynamic conditions by adding the integral to the left-hand side of Eq. (2).Variables B and T stand for the body force and the traction force on volume V and surface S respectively, ε and σ stand for strain and stress, respectively, while δ is the variation symbol. Thus at time t for a virtual displacement field δui consistent with the constraint conditions present, the relation can be extended as follows

$$-\iiint_V (\partial^2 u_i / \partial t^2) \, \delta u_i dV + \iiint_V B_i \delta u_i dV + \oiint_S T_i^{(n)} \delta u_i dS - \iiint_V \sigma_{ij} \delta \varepsilon_{ij} dV = 0 \tag{3}$$

This is a statement of the principle of virtual work, with inertia included as a distributed body force. In general, the displacement vector at a point has six components or displacement degrees of freedom

$$\{u\} = \begin{Bmatrix} u & v & w & \theta_x & \theta_y & \theta_z \end{Bmatrix}^T \tag{4}$$

Thus Eq. (2.2.3) can be rewritten in the matrix form as follows:

$$-\iiint_V \{\delta u\}^T [\rho] \{\ddot{u}\} dV + \iiint_V \{\delta u\}^T \{B\} dV + \oiint_S \{\delta u\}^T \{T\} dS - \iiint_V \{\delta \varepsilon\}^T \{\sigma\} dV = 0 \tag{5}$$

The structural displacement at any point on the domain could be approximated as

$$\{u\} = [N]\{d\} \tag{6}$$

where, {d} is an array containing displacements at certain predefined points on the structure, called nodes, [N] is an array of interpolation functions, and {u}is the array of displacements at any desired point on the structure, interpolated from the nodal displacements. The interpolation functions, [N], are assumed to be spatial functions whereas the nodal displacements, {d}, are temporal functions. Terms in Eq. (6) can be spatially differentiated to obtain strain versus nodal displacement relation, given by

$$\{\varepsilon\} = [B]\{d\} \tag{7}$$

The constitutive relation may be written as

$$\{\sigma\} = [D]\{\varepsilon\} \tag{8}$$

The detail expressions for the [B] and [D] matrices will be presented later. Thus, including the viscous damping, Eq. (5) becomes

$$-\iiint_V \{\delta d\}[N]^T[\rho][N]\{\ddot{d}\}\,dV + \iiint_V \{\delta d\}^T[N]^T\{B\}\,dV + \oiint_S \{\delta d\}^T[N]^T\{T\}\,dS - \iiint_V \{\delta d\}^T[B]^T[D][B]\{d\}\,dV = 0 \tag{9}$$

Since the virtual displacement {δd} is arbitrary, the governing equation of the system is

$$[M]\{\ddot{d}\} + [K]\{d\} = \{F\} \tag{10}$$

where,

$$[M] = \iiint_V [N]^T[\rho][N]\,dV$$ = Mass matrix, (11)

$$[K] = \iiint_V [B]^T[D][B]\,dV$$ = Stiffness matrix, (12)

and, $$\{F\} = \iiint_V [N]^T\{B\}dV + \oiint_S [N]^T\{T\}dS$$ = Force vector. (13)

Thus, to summarise, the governing equations for free vibration problem is furnished below:

$$[M]\{\ddot{d}\} + [K]\{d\} = \{0\} \tag{14}$$

3.1.1 Governing Equations of Lamina:

3.1.1.1 Basic Constitutive Equations:

From the law of conservation of linear momentum, the equations of motion are given by:

$$\sigma_{ij,i} + b_j = \rho\ddot{u}_j \tag{15}$$

From the law of conservation of angular momentum, one may obtain

$$\sigma_{ij} = \sigma_{ji} \tag{16}$$

Constitutive relation of general linear anisotropic material is given by

$$\sigma_{ij} = C_{ijkl}\,\varepsilon_{kl} \tag{17}$$

Combining above equations, and neglecting body force terms, equation of dynamic equilibrium may be represented as

$$\rho \ddot{u}_i - (C_{ijkl}\, \varepsilon_{kl})_j = 0 \quad (18)$$

Since σ_{ij} is symmetrical, C_{ijkl} must be symmetrical in i and j i.e.

$$C_{ijkl} = C_{jikl} \quad (19)$$

Again for linear elastic problems, the strain tensor, given by $\varepsilon_{kl} = 0.5(u_{k,l} + u_{l,k})$, is also symmetrical in l and k, therefore,

$$C_{ijkl} = C_{ijlk} \quad (20)$$

Using strain energy density function, W, defined as the strain energy contained in a unit volume of the structure undergoing deformation from an arbitrary datum, and given by

$$W = \frac{1}{2} C_{ijkl}\, \varepsilon_{ij}\, \varepsilon_{kl} \quad (21)$$

It can be obtained from mathematical identity

$$\frac{\partial^2 W}{\partial \varepsilon_{ij} \varepsilon_{kl}} = \frac{\partial^2 W}{\partial \varepsilon_{ijkl} \varepsilon_{ij}} \quad (22)$$

that, $C_{ijkl} = C_{klij}$. Finally it can be concluded that,

$$C_{ijkl} = C_{klij} = C_{jikl} = C_{ijlk} \quad (23)$$

Now it can be shown that in general anisotropic element among the 81 elastic constant, 21 are independent elastic constants.

Now the constitutive relationship can be written in pseudo-tonsorial form, with 21 material constants, as

$$\begin{Bmatrix} \sigma_1 \\ \sigma_2 \\ \sigma_3 \\ \sigma_4 \ or\ \tau_{23} \\ \sigma_5 or\ \tau_{13} \\ \sigma_6\ or\ \tau_{12} \end{Bmatrix} = \begin{bmatrix} c_{11} & c_{12} & c_{13}\, c_{14} & c_{15} & c_{16} \\ c_{12} & c_{22} & c_{23}\, c_{24} & c_{25} & c_{26} \\ c_{13} & c_{23} & c_{33}\, c_{34} & c_{35} & c_{36} \\ c_{14} & c_{24} & c_{34}\, c_{44} & c_{45} & c_{46} \\ c_{15} & c_{25} & c_{35}\, c_{45} & c_{55} & c_{56} \\ c_{16} & c_{26} & c_{36}\, c_{46} & c_{56} & c_{66} \end{bmatrix} \begin{Bmatrix} \varepsilon_1 \\ \varepsilon_2 \\ \varepsilon_3 \\ \varepsilon_4\ or\ \gamma_{23} \\ \varepsilon_5\ or\ \gamma_{13} \\ \varepsilon_6\ or\ \gamma_{12} \end{Bmatrix} \quad (24)$$

3.1.1.2 Elastic Stiffness Matrix:

Generally the constitutive relationship matrix Cij depend on the orientation of the co-ordinate system. An isotropic material is characterized by infinite number of planes of material symmetry through a point. An isotropic material is characterized by only two independent elastic constant, c11, c12.

$$\begin{Bmatrix} \sigma_1 \\ \sigma_2 \\ \sigma_3 \\ \sigma_4 \\ \sigma_5 \\ \sigma_6 \end{Bmatrix} = \begin{bmatrix} c_{11} & c_{12} & c_{12} & 0 & 0 & 0 \\ c_{12} & c_{11} & c_{12} & 0 & 0 & 0 \\ c_{12} & c_{12} & c_{11} & 0 & 0 & 0 \\ 0 & 0 & 0 & (c_{11} - c_{12})/2 & 0 & 0 \\ 0 & 0 & 0 & 0 & (c_{11} - c_{12})/2 & 0 \\ 0 & 0 & 0 & 0 & 0 & (c_{11} - c_{12})/2 \end{bmatrix} \begin{Bmatrix} \varepsilon_1 \\ \varepsilon_2 \\ \varepsilon_3 \\ \varepsilon_4 \\ \varepsilon_5 \\ \varepsilon_6 \end{Bmatrix}$$

In case of an orthotropic material, which has three mutually perpendicular plane of symmetry, number of independent elastic constant reduced to nine. For orthotropic material independent coefficients are c11, c12, c13, c22, c23, c33, c44, c55, c66.

$$\begin{Bmatrix}\sigma_1\\ \sigma_2\\ \sigma_3\\ \sigma_4\\ \sigma_5\\ \sigma_6\end{Bmatrix} = \begin{bmatrix} c_{11} & c_{12} & c_{13} & 0 & 0 & 0\\ c_{12} & c_{22} & c_{23} & 0 & 0 & 0\\ c_{13} & c_{23} & c_{33} & 0 & 0 & 0\\ 0 & 0 & 0 & c_{44} & 0 & 0\\ 0 & 0 & 0 & 0 & c_{55} & 0\\ 0 & 0 & 0 & 0 & 0 & c_{66}\end{bmatrix} \begin{Bmatrix}\varepsilon_1\\ \varepsilon_2\\ \varepsilon_3\\ \varepsilon_4\\ \varepsilon_5\\ \varepsilon_6\end{Bmatrix} \quad (25)$$

For an orthotropic material following reciprocal law holds:

$\frac{\nu_{ij}}{E_i} = \frac{\nu_{ji}}{E_j}$, (i, j=1, 2, 3)

The relation between the stiffness constant and the engineering constant for orthotropic material is given by:

c11= E1$\frac{1-\nu_{23}\nu_{32}}{\Delta}$, c12= E1$\frac{\nu_{21}-\nu_{31}\nu_{23}}{\Delta}$ = E2$\frac{\nu_{12}-\nu_{32}\nu_{13}}{\Delta}$

c12= E1$\frac{\nu_{31}-\nu_{21}\nu_{32}}{\Delta}$ = E3 $\frac{\nu_{13}-\nu_{12}\nu_{23}}{\Delta}$, c22= E2$\frac{1-\nu_{13}\nu_{31}}{\Delta}$ (26)

c23= E2$\frac{\nu_{32}-\nu_{12}\nu_{31}}{\Delta}$ = E3 $\frac{\nu_{23}-\nu_{21}\nu_{13}}{\Delta}$, c33= E3$\frac{1-\nu_{12}\nu_{21}}{\Delta}$

c44= G23, c55= G31, c66= G12,

Δ = 1– v12v21 –v23v32 –v31v13 –2v21v32 v13

Here, directions 1, 2 and 3 are directions of orthotropy

E1, E2, E3 = Young moduli in 1, 2 and 3 directions, respectively

vij= Poisson's ratio of transverse strain in the jth direction to the axial strain in the ith direction, when stressed in the ith direction.

= - εj / εi

G23, G13, G12 = shear moduli in the 2-3, 1-3 and 1-2 planes, respectively.

A fiber-reinforced composite lamina is essentially an orthotropic material, since the presence of fiber, say, along the direction 1, renders this direction more strength and stiffness compared to directions normal to it. However, a lamina being essentially a thin plate, plane stress assumptions apply here quite adequately. Hence, the elastic relations may be simplified as follows:

Q11=$\frac{E_1}{1-\nu_{12}\nu_{21}}$, Q22= $\frac{E_2}{1-\nu_{12}\nu_{21}}$, Q12= v12 Q22 = v21 Q11, (27)

Q44= G23, Q55= G31, Q66= G12

In general, though the transverse shear stresses σ4 (or τ23) and σ5 (or τ31), are not incorporated in plane stress analysis, here these stresses are accounted so that the Mindlin's plate theory may be used instead of the conventional Kirchhoff's theory. In matrix form

$$\begin{Bmatrix}\sigma_1\\ \sigma_2\\ \sigma_4\\ \sigma_5\\ \sigma_6\end{Bmatrix} = \begin{bmatrix}Q_{11} & Q_{12} & 0 & 0 & 0\\ Q_{12} & Q_{22} & 0 & 0 & 0\\ 0 & 0 & Q_{44} & 0 & 0\\ 0 & 0 & 0 & Q_{55} & 0\\ 0 & 0 & 0 & 0 & Q_{66}\end{bmatrix}\begin{Bmatrix}\varepsilon_1\\ \varepsilon_2\\ \varepsilon_4\\ \varepsilon_5\\ \varepsilon_6\end{Bmatrix} \quad (28)$$

Above matrix is decomposed in to two parts and the stress strain relations is rewritten in the principal material direction 1, 2, and 3 as follows:

$$\begin{Bmatrix}\sigma_1\\ \sigma_2\\ \sigma_6\end{Bmatrix} = \begin{bmatrix}Q_{11} & Q_{12} & 0\\ Q_{12} & Q_{22} & 0\\ 0 & 0 & Q_{66}\end{bmatrix}\begin{Bmatrix}\boldsymbol{\varepsilon_1}\\ \boldsymbol{\varepsilon_2}\\ \boldsymbol{\varepsilon_3}\end{Bmatrix}$$

and $\begin{Bmatrix}\sigma_4\\ \sigma_5\end{Bmatrix} = \begin{bmatrix}Q_{44} & 0\\ 0 & Q_{55}\end{bmatrix}\begin{Bmatrix}\varepsilon_4\\ \varepsilon_5\end{Bmatrix}$ (29)

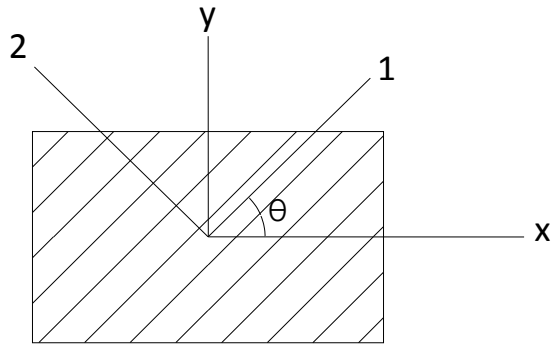

Figure 3.1 Arbitrarily oriented Lamina

The stress σz or σ3 has been dropped in the Mindlin's theory. The off axis stress strain relations of the lamina, with respect to the x, y and z axes (Fig.3.1) are expressed as

$$\begin{Bmatrix}\sigma_x\\ \sigma_y\\ \sigma_{xy}\end{Bmatrix} = \begin{bmatrix}Q'_{11} & Q'_{12} & Q'_{16}\\ Q'_{12} & Q'_{22} & Q'_{26}\\ Q'_{16} & Q'_{12} & Q'_{66}\end{bmatrix}\begin{Bmatrix}\varepsilon_x\\ \varepsilon_y\\ \varepsilon_{xz}\end{Bmatrix} \quad (30)$$

and $\begin{Bmatrix}\sigma_{xz}\\ \sigma_{yz}\end{Bmatrix} = \begin{bmatrix}Q'_{44} & Q'_{45}\\ Q'_{45} & Q'_{55}\end{bmatrix}\begin{Bmatrix}\varepsilon_{xz}\\ \varepsilon_{yz}\end{Bmatrix}$

The above equation is based on the assumption that the fibres are oriented along the direction 1, while the lamina lies on the 1-2 plane, directions 1 and 2 being mutually perpendicular. These relations are termed as the on-axis relations. The off-axis relations are obtained by operating suitable transformations on the on-axis relations. The off-axis relations are transformations needed to get the stress-strain relations along the local axes defined on the plate (Fig. 3.2):

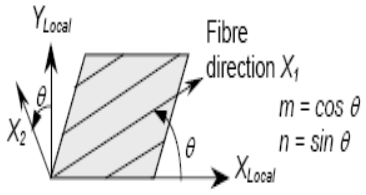

Figure 3.2 The orthotropic directions and local plate axes. The angle θ is termed as the fibre angle.

The elastic coefficients transformed from the orthotropic axes to the user-defined local co-ordinates are written with primes to identify them properly. These transformation rules in explicit form may be written as furnished below:

Where,

$$Q'11 = m4Q11 + 2m2n2\,(Q12+2Q66) + n4Q22$$

$$Q'22 = n4Q11 + 2m2n2\,(Q12+2Q66) + m4Q22$$

$$Q'12 = m2n2\,(Q11+ Q12 - 4Q66) + (m4 + n4)\,Q12$$

$$Q'16 = m3n\,(Q11- Q12 - 2Q66) - mn3\,(Q22 - Q12 - 2Q66) \quad (31)$$

$$Q'26 = mn3\,(Q11 - Q12 - 2Q66) - m3n\,(Q22- Q12 - 2Q66)$$

$$Q'66 = m2n2\,(Q11+ Q22 - 2Q12) + (m2 - n2)\,Q66$$

$$Q'44 = m2Q44 + n2Q55$$

$$Q'45 = mn\,(Q55 - Q44)$$

$$Q'55 = m2Q55 + n2Q44$$

3.1.2. Governing Equations of the Laminate:

General construction of laminated composite plate of thickness t consisting of unidirectional lamina bonded together to act as an integral continuum, is pictorially explained in Fig.3.3. The bond are infinitesimally thin and are not shear deformable. Hence, the displacements are continuous through the thickness of the laminate. In the present analysis the first order transverse shear deformation is assumed. Thus a vertical plane cross section before deformation is assumed to remain plane after deformation but it may not remain normal to the middle surface as it happens with the Kirchhoff's plates.

The following assumption is made according to the Yang-Norris-Stavsky (YNS) theory [7] which is a generalization of the Mindlin theory to accommodate composite laminates:

1. The material behavior is linear and elastic.

2. The thickness, t, of the laminate is small compared to the other two dimensions.

3. Displacements u, v, and W are small compared to the laminate thickness, h.

4. Normal to the mid-plane before deformation remains straight but not necessarily normal to the mid-plane after deformation.

5. Stresses normal to the mid-plane are neglected.

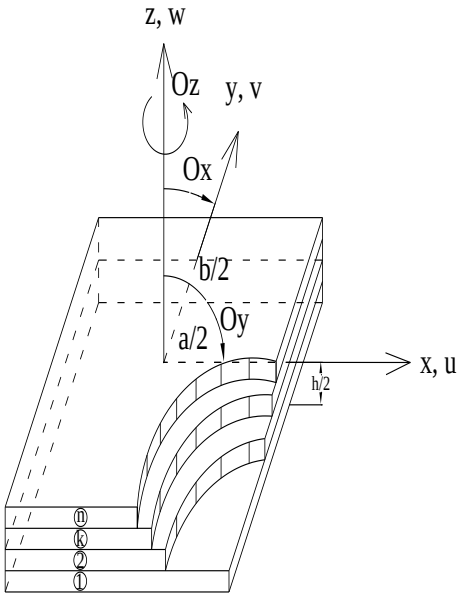

Figure 3.3 Laminated composite plate with positive displacements, rotations

3.1.2.1 Displacement Model:

The deformed geometry of the laminated plate is shown in Fig. 3.4 and Fig. 3.5. The displacement model adopted for flat plates in the present analysis includes the in-plane displacements u0and v0 at the mid-plane, an out-of-plane displacement w0, of the mid-plane and two rotations θx and θy as shown in Figs. 3.4 and 3.5.It may so happen that the vertical plane before bending is no longer perpendicular to the middle surface after deformation. Again, the mid-plane may have in-plane translations too. The total rotation is the sum of the shear rotation and bending rotation, as expressed in Eq. 21. The in-plane displacements and are assumed to vary linearly with depth, proportional to the total rotation, plus the mid-plane displacement, whereas, the transverse deflection is an invariant through the depth according to the assumptions of the YNS theory.

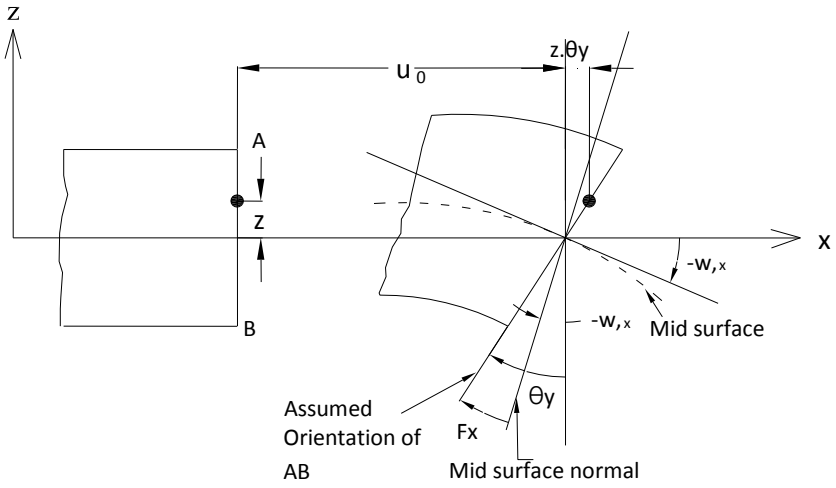

Figure 3.4 A 2-dimensional view of deformation of the plate along a section parallel to the x-z plane

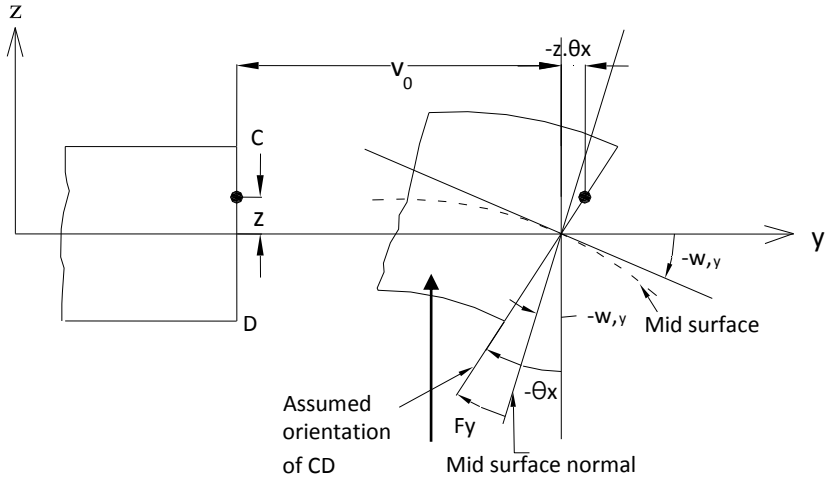

Figure 3.5 A 2-dimensional view of deformation of the plate along a section parallel to the y-z plane

The in-plane displacements u and v of any point at a distance z from the mid-plane for a Mindlin-composite plate are given by:

$u(x, y, z, t) = u0 + z\theta y\ (x, y, t)$

$v(x, y, z, t) = v0 - z\theta x\ (x, y, t)$ (32)

$w(x, y, z, t) = w0(x, y, t)$

The shear rotation of the plate can be expressed as

$\phi x = \theta y + w,x \quad , \phi y = -\theta x + w,y$ (33)

Withholding the spatial and temporal co-ordinates, for a Mindlin plate the following relations may be assumed for the displacement model:

$$\begin{Bmatrix} u \\ v \\ w \end{Bmatrix} = \begin{Bmatrix} u_0 + z\theta_y \\ v_0 - z\theta_x \\ w_0 \end{Bmatrix} \quad \text{and} \quad \begin{Bmatrix} \theta_x \\ \theta_y \end{Bmatrix} = \begin{Bmatrix} w,_y - \phi_y \\ -w,_x + \phi_x \end{Bmatrix} \tag{34}$$

The displacements of the flat plate are fully described by five components, u, v, w, θx and θy, where u, v and w are displacements along the x, y and z-directions and θx and θy are the linear rotations of initially vertical planes on the x-z and y-z planes after distortion, at location (x, y) on the mid-plane. The positive sign conventions for displacements and stress resultants are illustrated in Fig. 3.3. The mid-plane displacements in the x-, y- and z-direction are u0, v0, w0 (refer Figs. 3.4 and 3.5).With the displacements defined in Eq. (34), now the strains may be defined in terms of displacements. This kinematic relationship will be taken up in the next section. The definitions will be restricted within linear elastic zone however.

3.1.2.2 Strain-Displacement Relations

The linear in-plane strain of laminate at a distance z from the mid-surface are given by,

$$\varepsilon x = u,x = u0,x + z\,\theta y,x = \varepsilon 0x + z\kappa x$$

$$\varepsilon y = v,y = v0,y - z\,\theta x,y = \varepsilon 0y + z\kappa y \tag{35}$$

$$\varepsilon xy = u,y + v,x = u0,y + v0,x + z(\theta y,y - \theta x,x) = \varepsilon 0xy + z\kappa xy$$

Since, the transverse shear deformation is assumed same across the thickness of the laminate are given by,

$$\varepsilon xz = \phi x = \varepsilon 0xz, \quad \varepsilon yz = \phi y = \varepsilon 0xz \tag{36}$$

Substituting equation (35), (36) in equation (30), the stress in any lamina k can be expressed in terms of the laminate mid-surface strains, curvatures and shear rotations of the lamina.

$$\begin{Bmatrix} \sigma_x \\ \sigma_y \\ \sigma_{xy} \end{Bmatrix} = \left[Q'_{ij}\right]_k \begin{Bmatrix} \varepsilon_x^0 + z\kappa_x \\ \varepsilon_y^0 + z\kappa_y \\ \varepsilon_{xy}^0 + z\kappa_{xy} \end{Bmatrix} \quad \text{(i, j = 1, 2, 6)}$$

$$\begin{Bmatrix} \sigma_{xz} \\ \sigma_{yz} \end{Bmatrix} = \alpha \left[Q'_{ij}\right]_k \begin{Bmatrix} \phi_x \\ \phi_y \end{Bmatrix} \quad \text{(i, j = 4, 5)} \tag{37}$$

And α is a shear correction factor, taken as 5/6, to taken to account for the non-uniform distribution of the transverse shear strain across the thickness of the laminate.

3.1.2.3 Constitutive Relations for a Laminated Composite Plate:

The internal force and moment resultants of the laminate are obtained by integrating the lamina stresses over the entire plate thickness. Thus stress terms are replaced by the stress-resultant terms, while the conventional strain terms are replaced by the mid-plane strain terms. Thus, assuming that the laminate comprises of n laminae, for the in-plane force,

$$\begin{bmatrix} N_x \\ N_y \\ N_{xy} \end{bmatrix} = \int_{-t/2}^{t/2} \begin{bmatrix} \sigma_x \\ \sigma_y \\ \sigma_{xy} \end{bmatrix}_k dz = \sum_{k=1}^{n} \int_{z_{k-1}}^{z_k} \begin{bmatrix} \sigma_x \\ \sigma_y \\ \sigma_{xy} \end{bmatrix}_k \text{dz}$$

$$= \sum_{k=1}^{n} \int_{z_{k-1}}^{z_k} {Q'}_{ij}^{k} [e]_{x,y} \text{ dz}$$

$$= \sum_{k=1}^{n} \int_{z_{k-1}}^{z_k} {Q'}_{ij}^{k} ([\varepsilon^0]_{x,y} + [z\kappa]_{x,y}) \text{ dz}$$

$$\begin{bmatrix} M_x \\ M_y \\ M_{xy} \end{bmatrix} = \int_{-t/2}^{t/2} \begin{bmatrix} \sigma_x \\ \sigma_y \\ \sigma_{xy} \end{bmatrix}_k z dz = \sum_{k=1}^{n} \int_{z_{k-1}}^{z_k} \begin{bmatrix} \sigma_x \\ \sigma_y \\ \sigma_{xy} \end{bmatrix}_k z\text{dz}$$

$$= \sum_{k=1}^{n} \int_{z_{k-1}}^{z_k} z\, {Q'}_{ij}^{k} [\varepsilon]_{x,y} \text{dz}$$

$$= \sum_{k=1}^{n} \int_{z_{k-1}}^{z_k} {Q'}_{ij}^{k} ([z\varepsilon^0]_{x,y} + [z^2\kappa]_{x,y})\, dz$$

$$\begin{bmatrix} Q_x \\ Q_y \end{bmatrix} = \int_{-t/2}^{t/2} \begin{bmatrix} \sigma_{xz} \\ \sigma_{yz} \end{bmatrix}_k dz = \sum_{k=1}^{n} \int_{z_{k-1}}^{z_k} \begin{bmatrix} \sigma_{xz} \\ \sigma_{yz} \end{bmatrix}_k \text{dz} \quad (38)$$

$$= \sum_{k=1}^{n} \int_{z_{k-1}}^{z_k} \alpha \left[{Q'}_{ij}^{k} \right]_k \begin{Bmatrix} \varepsilon_{xz} \\ \varepsilon_{yz} \end{Bmatrix}_k \text{dz}$$

$$= \begin{bmatrix} A_{44} & A_{45} \\ A_{45} & A_{55} \end{bmatrix} \begin{Bmatrix} \varepsilon_{xz} \\ \varepsilon_{yz} \end{Bmatrix}_k$$

From equations (26), the internal force and moment resultants can be expressed as,

$$\{F\} = [D]\{\varepsilon\} \quad (39)$$

Where, {F} = {Nx, Ny, Nxy, Mx, My, Mxy, Qx, Qy }T

{ε}= { εx, εy, εxy, κx, κy, κxy, ϕx,ϕy}T = { εx, εy, εxy, κx, κy, κxy, εxz,εyz}T

$$[D] = \begin{bmatrix} A_{11} & A_{12} & A_{16} & B_{11} & B_{12} & B_{16} & 0 & 0 \\ A_{12} & A_{22} & A_{26} & B_{12} & B_{22} & B_{26} & 0 & 0 \\ A_{16} & A_{26} & A_{66} & B_{16} & B_{26} & B_{66} & 0 & 0 \\ B_{11} & B_{12} & B_{16} & D_{11} & D_{12} & D_{16} & 0 & 0 \\ B_{12} & B_{22} & B_{26} & D_{21} & D_{22} & D_{26} & 0 & 0 \\ B_{16} & B_{26} & B_{66} & D_{16} & D_{26} & D_{66} & 0 & 0 \\ 0 & 0 & 0 & 0 & 0 & 0 & A_{44} & A_{45} \\ 0 & 0 & 0 & 0 & 0 & 0 & A_{45} & A_{55} \end{bmatrix}$$

The stiffness of the laminate are

(Aij, Bij, Dij) = $\sum_{k=1}^{n} \int_{z_{k-1}}^{z_k} {Q'}_{ij}^{k} [1, z, z^2]_k dz$ (i, j = 1, 2 and 6)

(Aij) = $\alpha \sum_{k=1}^{n} \int_{z_{k-1}}^{z_k} {Q'}_{ij}^{k} dz$ (i, j = 4, 5) (40)

3.1.2.4 Principle of Total Potential Energy:

The potential energy of deformation of a laminated plate is given by

U = $\frac{1}{2} \iint_A \{\varepsilon\}^T [D] \{\varepsilon\} dA.$ (41)

The potential energy of inertia force and moment is expressed as

Vi = $- \iint_A \{u\}^T \{X\} dA.$ (42)

where, {X} = {pu0ω2n, pv0ω2n, pwω2n, Iθxω2n, Iθyω2n,}T

in which,

p = $\sum_{k=1}^{n} (z_k - z_{k-1}) \rho_k$, I = $\frac{1}{2} \sum_{k=1}^{n} (z_k^2 - z_{k-1}^2) \rho_k$

The total potential energy in respect of free vibration of laminated plates in is

∏ = U + Vi (43)

According to the principle of total potential Energy the first variation of ∏ in equation (43) is stationary for the equilibrium of laminated plate. Thus by equating δ∏ to zero in equations (43), the respective equilibrium conditions are obtained.

3.1.2.5 Equations of Motion

For any three-dimensional object the equations of motion is given by

$$\sigma_{ji,j} + B_i = \rho \ddot{u}_i \quad (44)$$

where, σij stand for the stress components, Bi for the body force components, ρ is the mass density and $\ddot{u}_i$ are the acceleration components of the structure. In the absence of body force, eq.(44) can be expanded as

$$\begin{aligned} \sigma_{x,x} + \tau_{yx,y} + \tau_{zx,z} &= \rho \ddot{u} \\ \tau_{xy,x} + \sigma_{y,y} + \tau_{zy,z} &= \rho \ddot{v} \\ \tau_{xz,x} + \tau_{yz,y} + \sigma_{z,z} &= \rho \ddot{w} \end{aligned} \quad (45)$$

Substituting the expanded form of u, v and w

$$\sigma_{x,x} + \tau_{yx,y} + \tau_{zx,z} = \rho(\ddot{u}_0 + z\ddot{\theta}_x) \tag{46a}$$

$$\tau_{xy,x} + \sigma_{y,y} + \tau_{zy,z} = \rho(\ddot{v}_0 + z\ddot{\theta}_y) \tag{46b}$$

$$\tau_{xz,x} + \tau_{yz,y} + \sigma_{z,z} = \rho\ddot{w}_0 \tag{46c}$$

From integration of Eq (46a) over depth z = ± h/2, it is obtained that

$$\int_{-h/2}^{h/2} \sigma_{x,x} dz + \int_{-h/2}^{h/2} \tau_{yx,y} dz + \int_{-h/2}^{h/2} \tau_{zx,z} dz = \int_{-h/2}^{h/2} \ddot{u}_0 dz + \int_{-h/2}^{h/2} z\rho\ddot{\theta}_x dz$$

$$or,\ N_{x,x} + N_{yx,y} + \tau_{zx}\Big|_{-h/2}^{h/2} = \ddot{u}_0 \int_{-h/2}^{h/2} \rho\, dz + \ddot{\theta}_x \int_{-h/2}^{h/2} z\rho\, dz$$

$$or,\ N_{x,x} + N_{yx,y} + 0 = I\ddot{u}_0 + P\ddot{\theta}_x;\ I = \int_{-h/2}^{h/2} \rho\, dz; P = \int_{-h/2}^{h/2} \rho\, z\ dz \tag{47}$$

The third term in the left-hand-side is taken to zero since the transverse shear at top and bottom of the plate structures are identically zero. Similar treatment to (46b) produces

$$N_{xy,x} + N_{y,y} + 0 = I\ddot{v}_0 + P\ddot{\theta}_y;\ I = \int_{-h/2}^{h/2} \rho\, dz; P = \int_{-h/2}^{h/2} \rho\, z\ dz \tag{48}$$

Finally, from (46c), upon integration over depth the third equation of motion is found:

$$Q_{x,x} + Q_{y,y} + q = \ddot{w}_0 I \tag{49}$$

Two more equations of motion can be obtained by multiplying both sides of Eqs. (46a) and (46b) by depth co-ordinate z and integrating over the thickness. Thus,

$$\int_{-h/2}^{h/2} \sigma_{x,x} z dz + \int_{-h/2}^{h/2} \tau_{yx,y} z dz + \int_{-h/2}^{h/2} \tau_{zx,z} z dz = \int_{-h/2}^{h/2} \rho\ddot{u}_0 z dz + \int_{-h/2}^{h/2} z^2 \rho\ddot{\theta}_x dz$$

$$or,\ M_{x,x} + M_{yx,y} - Q_x = \ddot{u}_0 \int_{-h/2}^{h/2} \rho\, z\, dz + \ddot{\theta}_x \int_{-h/2}^{h/2} z^2\ \rho\, dz$$

$$or,\ M_{x,x} + M_{yx,y} - Q_x = P\ddot{u}_0 + Q\ddot{\theta}_x;\ P = \int_{-h/2}^{h/2} \rho\, z\, dz; Q = \int_{-h/2}^{h/2} \rho\, z^2\ dz \tag{50}$$

Likewise, the last equation of motion is given by

$$M_{xy,x} + M_{y,y} - Q_y = P\ddot{v}_0 + Q\ddot{\theta}_y;\ P = \int_{-h/2}^{h/2} \rho z\, dz;\ Q = \int_{-h/2}^{h/2} \rho z^2\ dz \tag{51}$$

In matrix form the equation of motions for the Mindlin plate may be written as follows:

$$\begin{Bmatrix} N_{x,x} + N_{xy,y} \\ N_{xy,x} + N_{y,y} \\ Q_{x,x} + Q_{y,y} + q \\ M_{x,x} + M_{xy,y} - Q_x \\ M_{xy,x} + M_{y,y} - Q_y \end{Bmatrix} = \begin{bmatrix} I & 0 & 0 & P & 0 \\ 0 & I & 0 & 0 & P \\ 0 & 0 & I & 0 & 0 \\ P & 0 & 0 & Q & 0 \\ 0 & P & 0 & 0 & Q \end{bmatrix} \begin{Bmatrix} \ddot{u}_0 \\ \ddot{v}_0 \\ \ddot{w}_0 \\ \ddot{\theta}_x \\ \ddot{\theta}_y \end{Bmatrix};(I,P,Q) = \int_{-h/2}^{h/2} \rho(1, z, z^2) dz \tag{52}$$

or, $\{F\}=[\rho]\{A\}$, (53)

where {F} is the force vector, [ρ] is the inertia matrix, and {A} is the acceleration vector.

3.1.3 Finite Element Formulation:

The finite element formulation is based on the governing equation derived in section 3. The element stiffness, geometric stiffness and mass matrices are derived using the Principle of Total Potential Energy. A nine nodded Lagrangian isoparametric element have been used. Both the geometry and displacement field are expressed in terms of same shape functions. The parent element in local natural co-ordinate system can be mapped to an arbitrary shape in the Cartesian co-ordinate system. In Section 3 the expressions for the governing equations are derived with the assumption that the entire region of interest is a continuum. In finite element ideology, however, the continuum is visualised as an ensemble of finite number of user-defined elements, with finite number of nodes at their vertices, and the elements are connected to their neighbouring elements via the nodes only and not the interfaces. However, in general cases it is assumed that the elements boundaries do not separate or overlap, that is, the continuity is maintained throughout the continuum and inter-element interfaces. The intra-element properties are obtained from the nodal values, through interpolation functions, as described in Eq. (6). However, now the interpolation functions involve contributions only from the element nodes and not from all the structural nodes. This produces the same set of final outputs as in Eqs. (10), (11), (12), wherein the element mass and stiffness matrices are obtained. However, the integration over the depth of the plate are incorporated in the constitutive relations in an earlier stage (Section 3.1.2.3.), and hence the integrations are carried out over the area of the elements only with the help of Gauss Legendre quadrature. Thus the element matrices are given as below

$$[M_e] = \int_{-1}^{1}\int_{-1}^{1} [N]^T[\rho][N]|J|\, d\xi\, d\eta$$ = Mass matrix

$$[K_e] = \int_{-1}^{1}\int_{-1}^{1} [B]^T[D][B]|J| d\xi\, d\eta$$ = Stiffness matrix

and, $\{F_e\} = \int_{-1}^{1}\int_{-1}^{1} [N]^T \{T\}|J|\, d\xi\, d\eta$ = Force vector

Since we are dealing with free vibration analysis problem in this case the external Force vector [Fe] is zero as no external force acts on the system.

Here ξ and η are the element natural co-ordinates and |J| is the determinant of the

Jacobian matrix [J] = $\begin{bmatrix} \sum_{i=1}^{nel} \frac{\partial N_i}{\partial \xi} x_i & \sum_{i=1}^{nel} \frac{\partial N_i}{\partial \xi} y_i \\ \sum_{i=1}^{nel} \frac{\partial N_i}{\partial \eta} x_i & \sum_{i=1}^{nel} \frac{\partial N_i}{\partial \eta} y_i \end{bmatrix}$ (54)

nel being the number of nodes per element. The analyses are done in single dimensional storage arrays using Subspace iteration for Eigen problems.

3.1.3.1 Isoparametric Element:

The isoparametric means “same parameters” and is applied here because same interpolation functions are used to interpolate the magnitude of co-ordinates as well as the degree of freedom. If the interpolation functions for the degrees of freedom are of higher order than those used for co-ordinate interpolations, the element is called subparametric, while the reverse is the case for superparametric elements. By the use of isoparametric elements it is easier to simulate complicated geometries, while simplifying the computations simultaneously. A flat Mindlin-plate element, in general, has five displacement degrees of freedom at each node as shown in Eq. (30). Nine noded Lagrangian element [Fig 3.6.] with five degree of freedom at each node, i.e., u0, v0, w, θx, θy is considered for finite element formulation.

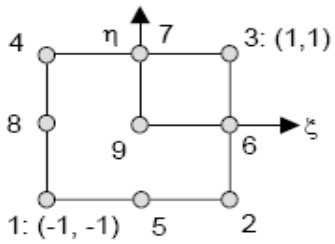

Figure 3.6 Nine-noded Lagrangian element

The co-ordinates and the elastic parameters inside an element can be interpolated using the shape functions and the nodal values as follows:

$$x_i = \sum_{j=1}^{NEL} N_j(\xi,\eta)(x_i)_j;\ i = 1,2,3$$

$$u_i = \sum_{j=1}^{NEL} N_j(\xi,\eta)(d_i)_j;\ i = 1,2,3,4,5 \qquad (55)$$

Here, NEL stands for nodes per element, whereas, ui stands for the five intra-element displacement components uo, vo, wo, θx, and θy at node i while di are the corresponding nodal displacements at node i, both considered at the middle surface of the plate.

The shape functions Nj in equations (55) are defined as

$N_j = (\xi 2 + \xi\xi_j)(\eta 2 + \eta\eta_j)/4;\ j = 1,2,3,4$

$N_j = \eta_j 2(\eta 2 - \eta\eta_j)(1 - \xi 2)/2 + \xi_j 2(\xi 2 - \xi\xi_j)(1 - \eta 2)/2;\ j = 5,6,7,8$ (56)

$N_j = (1 - \xi 2)(1 - \eta 2);\ j = 9$

Where ξ and η are the local natural co-ordinates of the element and ξj and ηj are the value of them at node j.

The strains at the mid-plane may be similarly written by taking the derivatives of the shape functions with respect to the spatial co-ordinates as shown below:

Since the shape functions, the elastic matrix, [D], and the inertia matrix, [ρ], are already known, as cited in Fig. (3.6) and Eqs. (39) and (52), the element stiffness and mass arrays can be easily computed in local axes using Eqs. (10) and (11). These element arrays are next transformed to fit the global axes before they are properly assembled. In the next section the transformation matrix is formed and the transformation to be applied over the element matrices is summarily discussed for completeness.

The derivatives of the shape functions Nj with respect to x and y are expressed in terms of their derivatives with respect to ξ and η by the following relationship:

$$\begin{pmatrix} N_{j,x} \\ N_{j,y} \end{pmatrix} = [J]^{-1} \begin{pmatrix} N_{j,\xi} \\ N_{j,\eta} \end{pmatrix}$$

Where, $[J] = \begin{bmatrix} x_{,\xi} & y_{,\xi} \\ x_{,\eta} & y_{,\eta} \end{bmatrix}$ = Jacobian matrix

The Principle of Total Potential Energy described in sec. 3.2.4 is applied for the element to derive the stiffness and mass matrices.

3.1.3.2 Element Stiffness Matrix:

The potential energy of deformation for the element, given by equation (29), is

$$U = \frac{1}{2}\iint_{Ae}\{\varepsilon\}^T[D]\{\varepsilon\}dA \quad (57)$$

if {ε} = [B]{δe} = [[B1] [B2] ……[B9]] {δe}

where {ε}= { εx εy εxy κx κy κxy εxz εyz}T

{δe} = {u01, v01, w1, θx1, θy1 …… u09, v09, w9, θx9, θy9}T

$$[Bi] = \begin{bmatrix} N_{i,x} & 0 & 0 & 0 & 0 \\ 0 & N_{i,y} & 0 & 0 & 0 \\ N_{i,y} & N_{i,x} & 0 & 0 & 0 \\ 0 & 0 & 0 & 0 & N_{i,x} \\ 0 & 0 & 0 & -N_{i,y} & 0 \\ 0 & 0 & 0 & -N_{i,x} & N_{i,y} \\ 0 & 0 & N_{i,x} & 0 & N_i \\ 0 & 0 & N_{i,y} & -N_i & 0 \end{bmatrix} (i = 1 \text{ to } 9)$$

then $U = \frac{1}{2}\int_{-a/2}^{a/2}\int_{-b/2}^{b/2}\{\delta e\}^T[B]^T[D][B]\{\delta e\}\,dx\,dy$ (58)

$$= \frac{1}{2}\int_{-a/2}^{a/2}\int_{-b/2}^{b/2}\{\delta e\}^T[K_e]\{\delta e\}$$

in which $[Ke] = \int_{-a/2}^{a/2}\int_{-b/2}^{b/2}[B]^T[D][B]dx\,dy$= element stiffness matrix. Since dx dy = |J| dξ dη, where |J| is the determinant of the Jacobian matrix, the element stiffness matrix can be expressed in local natural coordinates of the element. From equation (58),

$$[Ke] = \int_{-1}^{1}\int_{-1}^{1}[B]^T[D][B]|J|d\xi\,d\eta \quad (59)$$

3.1.4 Solution Process:

The minimization of ∏ in the equation (43) leads the following equilibrium conditions for the free vibration of the laminated plates.

([K] – ωn2 [M]) {δ} = 0

From which the natural frequencies are determined.

4 NUMERICAL RESULTS

4.1 Mesh convergence study

A mesh convergence study has been carried out to obtain minimum number of elements required to achieve the non-dimensional natural frequencies as accurately as possible optimizing the computation time. For this purpose, a square laminated composite plate is taken and analyzed under simply supported (SSSS) boundary conditions. The side-to-thickness ratio (=s/t) is taken as 100. Five mesh sizes containing 16(=4x4 mesh), 36(=6x6 mesh), 64(=8x8) 100(=10x10) and 144(=12x12) elements are considered for the convergence study. A similar study is then performed on the same plate with same physical properties and boundary conditions but with a 30^o skew angle. The material properties of the plate are as below-

Material property:

E_1	E_2	G_{12}	G_{23}	G_{13}	υ_{12}	υ_{21}	ρ
40x1011 N/m^2	$1x10^{11}$ N/m^2	60 Gpa	50 Gpa	60 Gpa	0.25	0.00625	1 kg/m^3

No. of layers: 5

Lay-up sequence: [45°/-45°/45°/-45°/45°]

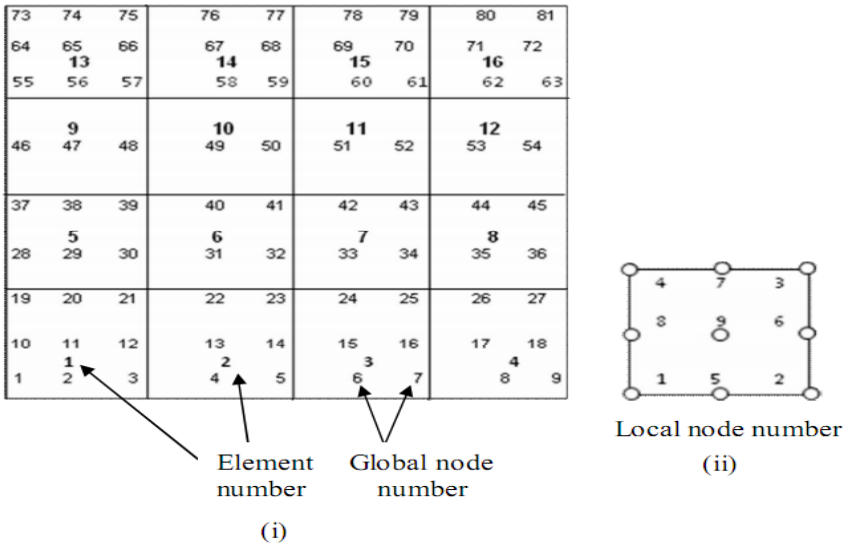

Figure 4.1 i) Element and node numbering for square plate ii) Local node numbering

The above figure depicts the node numbering for a 4x4 mesh which is used for convergence study. The non-dimensional frequencies for each of this mesh size are calculated using the formula given below,

$wi = wr*(2*\pi)*(\frac{s^2}{h})*(\sqrt{\frac{\rho}{E_2}})/\pi 2$

wi =non-dimensional frequency (radian/sec)

wr = natural frequency in hertz

s = dimension of the side of the square plate (in metre)

h = thickness of the plate (in metre)

ρ = density of the plate (Kg/m^3)

The results are presented in tabular form below in table No. 1 and 2. The first five modes are considered and available data in literature is also shown for reference: as reported by i) Wang and ii) Park Lee Voyiadjis.

Table 1: Normalized natural frequencies of square plates (0° skew angle) without cut out for SSSS condition and various element sizes

Elements	1st mode	2nd mode	3rd mode	4th mode	5th mode
4x4	12094.34	24912.56	30907.54	43130.34	53441.98
6x6	12064.10	24676.76	30544.70	42045.04	50943.46
8x8	12054.41	24634.65	30466.70	41841.42	50484.26
10x10	12049.67	24622.83	30439.10	41782.92	50352.17
12x12	12046.87	24618.53	30426.09	41761.30	50303.32

Table 2: Normalized natural frequencies of skew plates (30^o skew angle) without cut out for SSSS condition and various element sizes

Elements	1st mode	2nd mode	3rd mode	4th mode	5th mode
4x4	16307.13	32141.61	37697.48	53388.81	68839.68
6x6	15977.14	32219.34	37207.01	51765.59	64938.15
8x8	15918.07	32205.08	37108.68	51439.81	64215.02
10x10	15913.99	32190.72	37084.77	51355.44	64025.85
12x12	15911.70	32182.07	37069.23	51322.29	63950.08

It is clearly observed from the two tables that values of frequencies converge very well for all the five modes. As can be seen from both the preceding tables, the fundamental frequency converges for the 8x8 mesh having 64 elements, but for higher modes a refined mesh is required. For the fifth mode, the percentage difference between frequencies obtained for the mesh sizes 10x10 and 12x12 is 0.097 only in first table while it is 0.118 only in the second table. Hence, it is decided that the 10x10 elements meshing having 100 elements be taken for our further analysis since improvement in accuracy of the results in the 12x12 meshing is marginal and practically insignificant. Further, this will help to save computational resources.

4.2 Validation study

The Validation studies are performed to assess the accuracy and efficacy of the computer program which is used for carrying out the test by tallying it with results already there in the literature. Results from ANSYS (Release 15) for the same data and parameters for each case is also shown.

Study I: First of all, we present a table showing the difference in the results of analysis of our software program and those of Park Lee Voyiadjis as well as Wang for a fully clamped (CCCC) laminated composite plate 1mx1m size and 10 cm thickness and of the following material properties-

Material property

E_1	E_2	G_{12}	G_{23}	G_{13}	υ_{12}	υ_{21}	ρ
$40x10^{11}$ N/m^2	$1x10^{11}$ N/m^2	60 Gpa	50 Gpa	60 Gpa	0.25	0.00625	1 kg/m^3

No. of layers: 5

Lay-up sequence: [45^o/-45^o/45^o/-45^o/45^o]

In this case there is no central cutout but the skew angle varies. All frequencies are in radians. Results are obtained in terms of non-dimensional frequencies which is mathematically expressed as below-

$wi = wr*(2*\pi)*(\frac{s^2}{h})*(\sqrt{\frac{\rho}{E_2}})/\pi 2$

Wi =non-dimensional frequency

wr = natural frequency in hertz

s = dimension of the side of the square plate

h = thickness of the plate

ρ = density of the plate

Table 3: Normalized natural frequencies of skew plates of 10 cm thickness without cut out for CCCC condition

Skew angle	Mode	This study (FSDT)	Park Lee Voyiadjis (HSDT)	% difference	Wang (FSDT)	% difference	ANSYS 15 (FSDT)	% difference
0	1st	2.2858	2.3086	-1.00	2.2857	0.00	2.2336	2.28
	2nd	3.7402	3.7482	-0.21	3.7392	0.03	3.6595	2.16
	3rd	3.9824	4.0569	-1.87	3.9813	0.03	3.8671	2.90
	4th	5.1823	5.1631	0.37	5.1800	0.04	5.0625	2.31
	5th	5.7092	5.7649	-0.98	5.7019	0.13	5.5565	2.67
30	1st	2.6627	2.6260	1.38	2.6626	0.00	2.6133	1.86
	2nd	4.1379	4.0636	1.80	4.1367	0.03	4.0418	2.32
	3rd	4.7244	4.6501	1.57	4.7227	0.04	4.6337	1.92
	4th	5.4988	5.4037	1.73	5.4950	0.07	5.3524	2.66
	5th	6.5501	6.3307	3.35	6.5410	0.14	6.3966	2.34
45	1st	3.3526	3.2951	1.72	3.3523	0.01	3.2877	1.94
	2nd	4.8100	4.7067	2.15	4.8079	0.04	4.6987	2.31
	3rd	6.0545	5.9581	1.59	6.0520	0.04	5.9356	1.96
	4th	6.1093	5.9649	2.36	6.1029	0.11	5.9535	2.55
	5th	7.4312	7.2176	2.87	7.4069	0.33	7.2220	2.81

The comparison of results in Table 3 shows that the present results are in very close agreement with those of Wang (FSDT) and are reasonably close to those of Park Lee Voyiadjis (HSDT). Further, all our results are reasonably close to those from ANSYS 15 (FSDT). This is validation for a thick plate (side/thickness ratio of 10).

Study II: Now, we present a table showing the difference in the results of analysis of our software program and those of M.K. Singha, M. Ganapathi as well as Wang for a fully clamped (CCCC) laminated composite plate 1mx1m size and 10 mm thickness and of the same material properties and plate size as in study I.

Table 4: Normalized natural frequencies of skew plates of 10 mm thickness without cut out for CCCC condition

Skew angle	Mode	This study (FSDT)	M.K. Singha, M. Ganapathi (FSDT)	% difference	Wang (FSDT)	% difference	ANSYS 15 (FSDT)	% difference
0	1st	3.9010	3.8996	-0.04	3.9009	0.00	3.8478	-1.36
	2nd	7.1510	7.1426	-0.12	7.1464	-0.06	7.0189	-1.85
	3rd	8.4644	8.4532	-0.13	8.4585	-0.07	8.2661	-2.34
	4th	11.2291	11.2008	-0.25	11.2112	-0.16	10.9478	-2.51
	5th	13.3648	13.304	-0.46	13.3216	-0.32	12.9716	-2.94
	1st	4.5432	4.5425	-0.02	4.5431	0.00	4.4853	-1.27

30	2nd	8.3874	8.3787	-0.10	8.3819	-0.07	8.2252	-1.93
	3rd	9.8879	9.8764	-0.12	9.881	-0.07	9.6751	-2.15
	4th	12.8747	12.8428	-0.25	12.8533	-0.17	12.5145	-2.80
	5th	15.7341	15.6673	-0.42	15.6906	-0.28	15.3007	-2.75
45	1st	6.3051	6.2903	-0.24	6.3048	-0.01	6.2068	-1.56
	2nd	10.8302	10.7941	-0.33	10.8193	-0.10	10.5643	-2.46
	3rd	14.5085	14.4487	-0.41	14.4949	-0.09	14.1071	-2.77
	4th	15.5093	15.4235	-0.55	15.4692	-0.26	14.9933	-3.33
	5th	21.1720	20.9774	-0.92	21.062	-0.52	20.2726	-4.25

The comparison of results in Table 4 shows that the present results are in close agreement with those of Wang (FSDT) and are quite close to those of M.K. Singha, M. Ganapathi (FSDT). Further, all our results are reasonably close to those from ANSYS 15 (FSDT). This is validation for a thin plate (side/thickness ratio of 1000).

Study III: In order to validate our FEM code developed for free vibration analysis, the normalized natural frequency of a symmetric composite square laminate is computed and compared with the results reported by Kumar and Shrivastava and also by Park Lee Voyiadjis. Now we present another table showing comparison of analysis results of our study and Kumar and Shrivastava and also of Park Lee Voyiadjis for the first five modes for no skewness but variation of the central square cutout size. All frequencies are in radians. These results pertain to a simply supported (SSSS) laminated composite plate 1mx1m size and 1.333 cm thickness and of the following material properties-

E_1	E_2	G_{12}	G_{23}	G_{13}	υ_{12}	υ_{21}	ρ
$13x10^{10}$ N/mm^2	$1x10^{10}$ N/mm^2	5 Gpa	3.3 Gpa	5 Gpa	0.35	0.0269	1500 kg/m^3

No. of layers: 40

Lay-up sequence : $[(\pm 45^o/0^o{}_2)_3(90^o/0^o{}_2/90^o)_2]_s$

Figure 4.2 Node numbering for square plate with cut-out

Results are obtained in terms of non-dimensional frequencies which is mathematically expressed as below

$wi = wr*(2*\pi)*(\frac{s^2}{h})*(\sqrt{\frac{\rho}{E_2}})$

Wi =non-dimensional frequency
wr = natural frequency in hertz
s = dimension of the side of the square plate
h = thickness of the plate
ρ = density of the plate

Table 5: Normalized natural frequencies of simply supported square plates with centrally positioned square cutouts

cutout ratio (a/s = b/s)	source	1st mode	2nd mode	3rd mode	4th mode	5th mode
0	Kumar and Shrivastava (FSDT)	13.59	29.11	37.79	53.93	55.07
	Kumar and Shrivastava (HSDT)	13.71	29.5	38.3	54.85	55.97
	ANSYS 15	13.5947	29.0410	37.7178	53.6714	54.3815
	Park Lee Voyiadjis (HSDT)	13.59	29	37.66	53.6	-
	This study	13.5948	29.0448	37.7390	53.7014	54.4088
	% difference from Kumar and Shrivastava	-0.04	0.22	0.14	0.42	1.20
	% difference from ANSYS 15	0.00	-0.01	-0.06	-0.06	-0.05
0.2	Kumar and Shrivastava (FSDT)	13.15	28.3	35.79	52.4	55.3
	Kumar and Shrivastava (HSDT)	13.4	29.06	36.9	53.42	56.27
	ANSYS 15	12.6885	30.8720	31.5511	51.1503	63.5257
	Park Lee Voyiadjis (HSDT)	13.11	28.24	35.52	51.96	-
	This study	13.1286	28.2607	35.5412	52.1272	54.4380
	% difference from Kumar and Shrivastava	0.16	0.14	0.70	0.52	1.56
	% difference from ANSYS 15	-3.47	8.46	-12.65	-1.91	14.31
0.4	Kumar and Shrivastava (FSDT)	14.24	25.65	28.64	48.71	51.44
	Kumar and Shrivastava (HSDT)	14.86	26.68	29.91	49.76	54.1
	ANSYS 15	13.8246	26.1694	26.3464	46.3929	51.0773
	Park Lee Voyiadjis (HSDT)	14.17	25.64	28.6	48.26	-
	This study	14.2242	25.5881	28.5201	48.4497	50.9128
	% difference from Kumar and Shrivastava	0.11	0.24	0.42	0.53	1.02
	% difference from ANSYS 15	-2.89	2.22	-8.25	-4.43	0.32
0.6	Kumar and Shrivastava (FSDT)	19.52	28.2	29.37	45.22	51.65
	Kumar and Shrivastava (HSDT)	21.06	30.06	31.41	49.42	53.47
	ANSYS 15	19.6722	28.8694	29.0410	45.4436	52.8992
	Park Lee Voyiadjis (HSDT)	19.33	27.81	28.86	43.98	-
	This study	19.4114	27.8178	28.8832	43.8873	51.1058
	% difference from Kumar and Shrivastava	0.56	1.36	1.66	2.95	1.05
	% difference from ANSYS 15	1.33	3.64	0.54	3.42	3.39

Again it is clear that our results are in good agreement with the results of Park Lee Voyiadjis (HSDT) as well as with those of ANSYS 15 (FSDT) and closely agrees with the results of Kumar and Shrivastava (FSDT). It is clear that the results obtained using our computer program are reasonably accurate and quite acceptable.

4.3 Case studies

A series of parametric case studies has been conducted on the laminated composite plates with cut-out/skewness. Both external and internal parameters are varied to get a comprehensive idea about the effect variation due to skew angle, boundary conditions, thickness and cut out ratio on the dynamic behavior of laminated composite plates. The following case studies are provided-

1. Effect of variation due to skew angle without cut out
2. Effect of variation due to boundary conditions
3. Effect of variation due to thickness
4. Effect of variation due to cut out ratio
5. Effect of variation due to skew angle for cut out ratio 0.4

The Mechanical properties of the laminate that is considered for the study is given in the table below-

E_1	E_2	G_{12}	G_{23}	G_{13}	υ_{12}	υ_{21}	ρ
40x1011 N/m^2	$1x10^{11}$ N/m^2	60 Gpa	50 Gpa	60 Gpa	0.25	0.00625	1 kg/m^3

No. of layers: 5

Lay-up sequence: [45°/-45°/45°/-45°/45°]

The plate dimensions are 1mx1m with thickness of 10 mm.

4.3.1 Case study 1: Effect of variation due to skew angle without cut out

To study the effect of variation due to change in skew angle (without any cut out) on the natural frequency of the laminate, five skew angles – 0°, 15°, 30°, 45° and 60°are considered first for SSSS boundary condition and then for CCCC condition. The properties of the laminate, No. of layers, lay up sequence and dimensions of the plate are same as given in 4.3.

Frequencies pertaining to the first five modes are presented in the following tables where Table 6 data corresponds to results obtained under SSSS condition while those of Table 7 pertain to results obtained under CCCC condition.

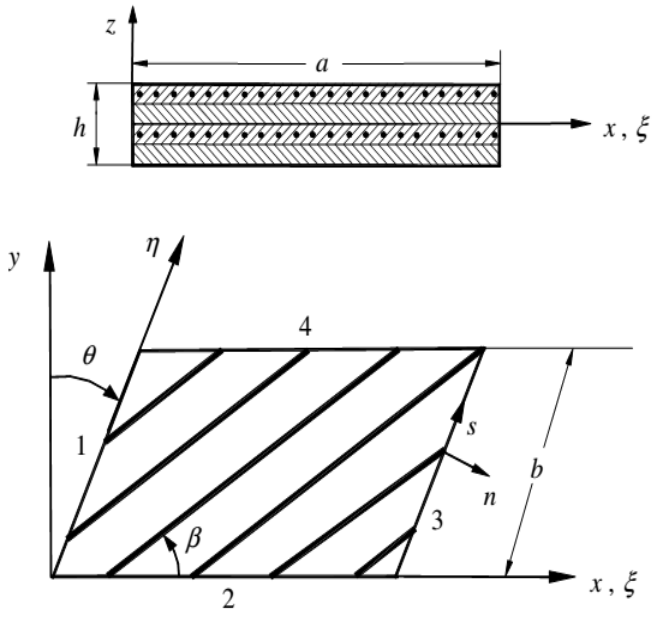

Figure 4.3 Skew plate geometry

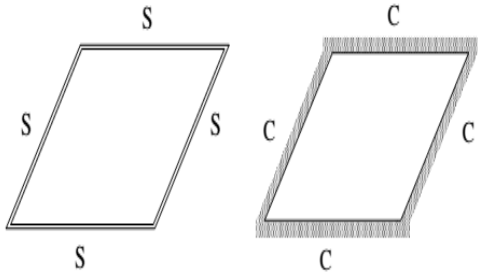

Figure 4.4 Illustration of two common boundary conditions

Table 6: Natural frequencies of SSSS skew plates without cut out

Mode→ Skew angle (°)↓	1st	2nd	3rd	4th	5th
0	12049.67	24622.83	30439.10	41782.92	50352.17
15	13166.40	28641.62	29471.20	48541.91	51509.83
30	15913.99	32190.72	37084.77	51355.44	64025.85
45	21223.31	39820.93	53792.35	59362.62	83170.76
60	39595.66	66190.86	90974.28	106016.69	119847.93

To visualize the effect of variation of skew angle on the free vibration behavior of composite plates in SSSS boundary condition, a graph is plotted below with the data of table 6. Each of the curves correspond to one of the modes.

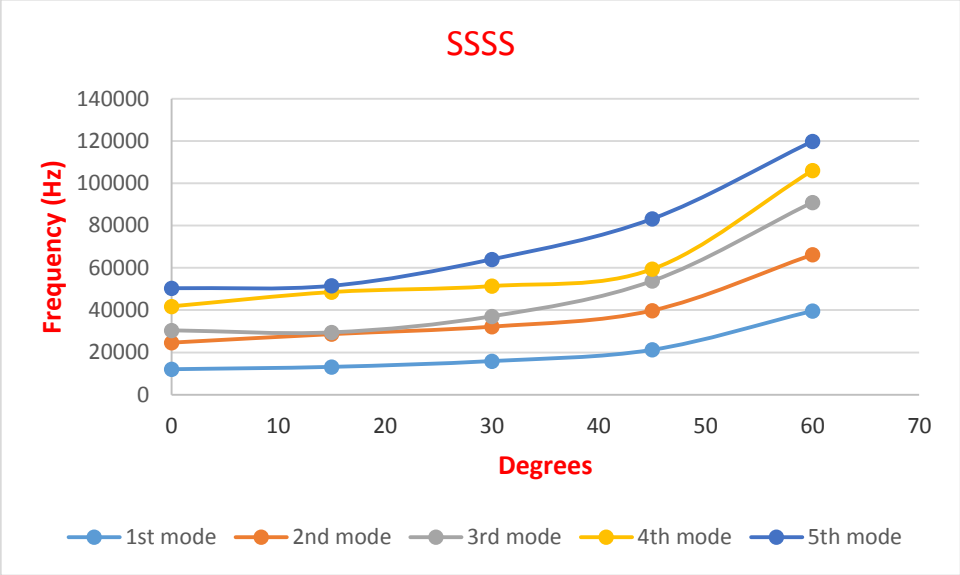

Figure 4.5 Variation of frequency with skew angle for a composite laminate having no cut-out for SSSS condition. First five modes shown.

Table 7: Natural frequencies of CCCC skew plates without cut out

Mode → Skew angle (°) ↓	1st	2nd	3rd	4th	5th
0	19132.62	34908.75	41132.46	54459.57	64571.58
15	19160.37	36642.85	39821.60	59665.07	62123.60
30	22297.62	40902.25	48122.55	62268.31	76091.14
45	30858.97	52551.86	70177.85	74624.93	100934.34
60	55421.15	84937.43	112484.96	131022.71	145102.34

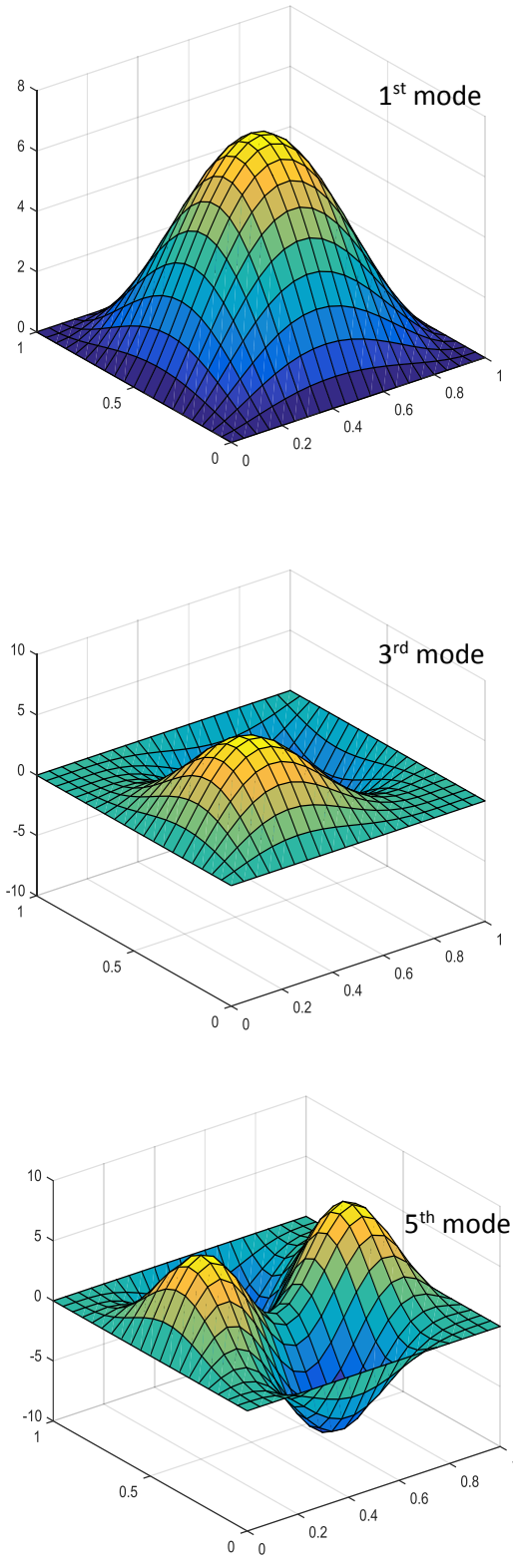

Fig. 4.5a First five mode shapes of a 1mx1m square plate of 10 mm thickness under CCCC boundary condition.

To visualize the effect of variation of skew angle on the free vibration behavior of composite plates in

CCCC boundary condition, a graph is plotted below with the data of table 7. Each of the curves correspond to one of the modes.

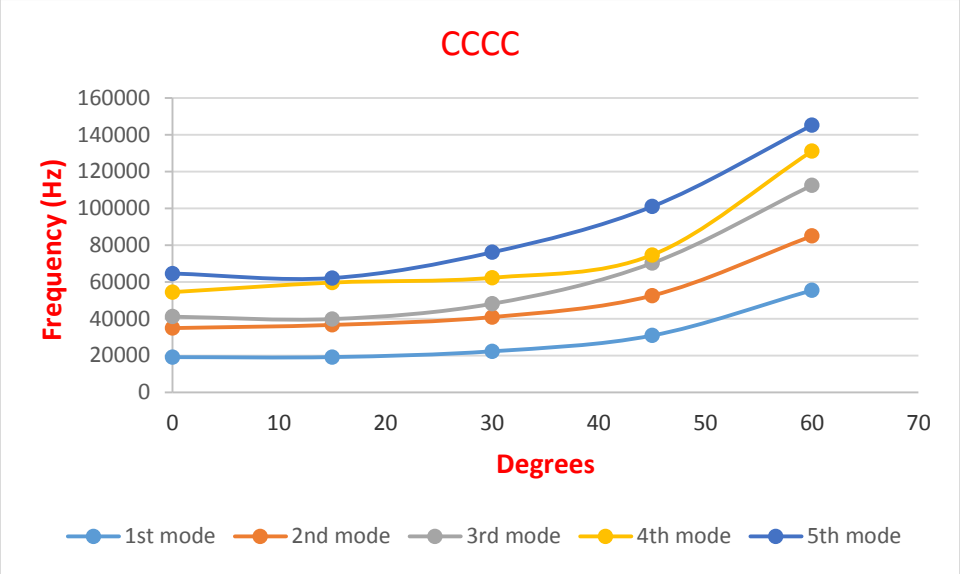

Figure 4.6 Variation of frequency with skew angle for a composite laminate having no cut-out for CCCC condition. First five modes shown.

To visualize the effect of variation of skew angle on the free vibration behavior of composite plates in SSSS and CCCC boundary conditions, a graph is plotted below with the data of table 6 and table 7. Only the first mode is shown so that the effect that change of boundary conditions may be highlighted.

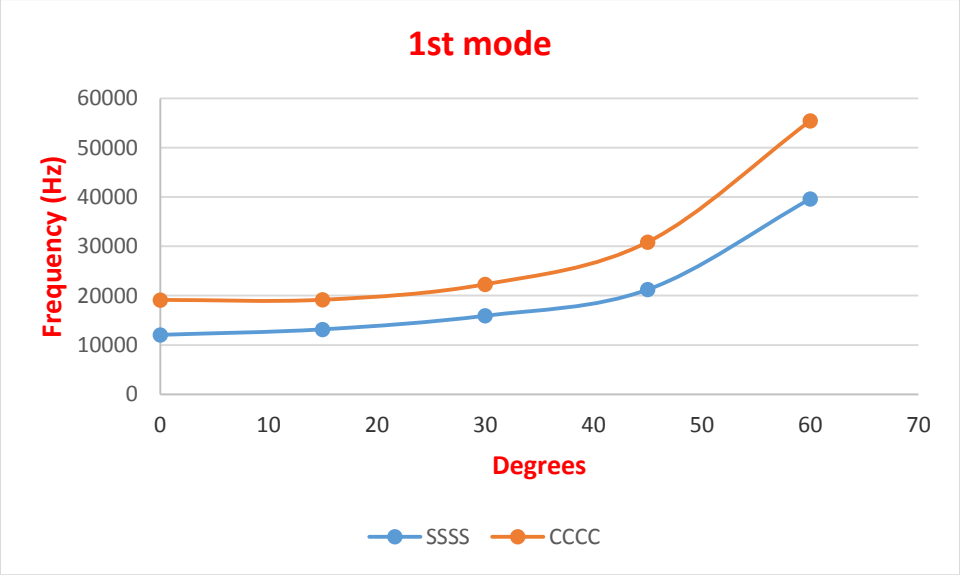

Figure 4.7 Variation of frequency with skew angle for a composite laminate having no cut out for SSSS and CCCC conditions. First mode only is shown.

Observations from the above tables and figures:

1. In both SSSS and CCCC cases there is a continuous increase in value of frequency with increase in skew angle (exception is fifth mode in SSSS condition) but for smaller values of skew angle, say up

to 30°, the percentage increase of frequency is not much whereas for higher values of skew angles like 45° or 60° the percentage increase of frequency is great. To illustrate this point let us take the case of increase of skew angle from 0° to 30° in CCCC where the corresponding increase of frequency is 16.54% in first mode but with increase in skew angle from 45° to 60°, the corresponding increase of frequency is79.59% for the same mode and boundary condition.

2. In both SSSS and CCCC cases the nature of curves is similar in general (with the exception of 4th mode) i.e. percentage increase of frequency between two consecutive values of skew angle is quite similar though this not strictly true for the third mode.
3. Though the nature of the curves for fundamental frequency for both SSSS and CCCC are very similar, the frequencies are always greater for the CCCC case.

4.3.2 Case study 2: Effect of variation due to boundary conditions

The effect of variation due to boundary conditions is studied by obtaining natural frequencies for five types of boundary condition namely SSSS, CCCC, CSCS, CCSS and CSSC. Skew angle is kept constant at 30° in each case. No cut out is considered. The properties of the laminate, No. of layers, lay up sequence and dimensions of the plate are same as given in 4.3. Results are summarised in Table 8.

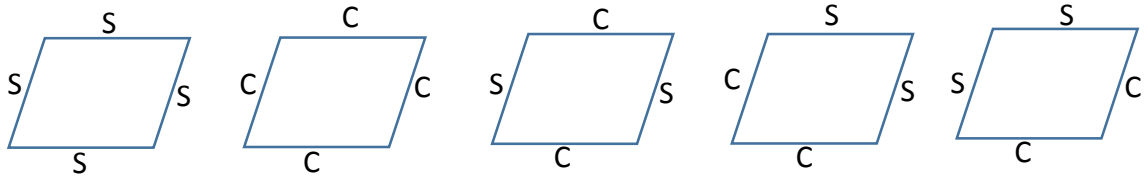

Figure 4.8 Illustration the of boundary conditions used in this study

Table 8: Natural frequencies of 30° skew plates under different boundary conditions

Mode→ Boundary Condition	1st	2nd	3rd	4th	5th
SSSS	15913.99	32190.72	37084.77	51355.44	64025.85
CCCC	22297.62	40902.25	48122.55	62268.31	76091.14
CSCS	20917.06	37338.52	46564.09	57920.25	69987.49
CCSS	18751.12	36602.95	41948.25	56642.59	70205.43
CSSC	18775.42	36592.76	42022.22	56628.65	70254.72

To depict the effect of change of boundary conditions on the free vibration behavior of composite plates, a bar chart is presented below with the data of table 8. Each of the bars correspond to one of the modes. For every mode, the frequency values obtained for the five different boundary conditions are depicted thus showing the effect of the variation.

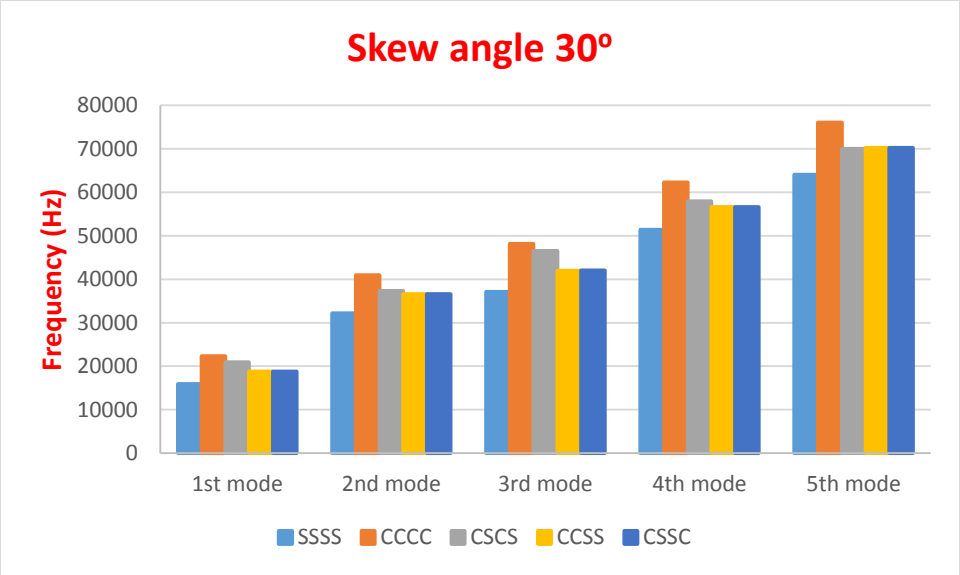

Figure 4.9 Variation of frequency with different boundary conditions for a 30° skew composite laminate having no cut-out. First five modes shown.

Observations from the above table and figure:

1. For every mode, the highest frequency is always from the CCCC condition and the lowest frequency is from the SSSS condition. One may infer that increasing the degree of constraints at the boundary has the effect of increasing the stiffness of the plate.
2. For the other three boundary conditions (CSCS, CCSS and CSSC) in this study the values of frequency in any particular mode are very close to one another.
3. One trend is that the percentage difference of frequencies between CCCC and SSSS conditions in a particular mode decreases more or less continuously from first mode (40.11) to fifth (18.84) mode.

4.3.3 Case study 3: Effect of variation due to laminate thickness

In order to study the effect of laminate thickness on the free vibration response, frequencies are obtained for five values of plate thickness namely 2 mm, 4mm, 6 mm, 8 mm and 10 mm against a skew angle of 15°. No cut out is considered now. In the first case all outer edges of the laminate are simply supported i.e. in SSSS condition and then in the second case all outer edges of the laminate are clamped i.e. in CCCC condition. The properties of the laminate, No. of layers, lay up sequence and other dimensions of the plate are same as given in 4.3. Results are shown in Tables 9 and 10 respectively.

Table 9: Natural frequencies of 15°skew plates under SSSS boundary condition without cut out for various plate thicknesses.

Mode→ Thickness (mm) ↓	1st mode	2nd mode	3rd mode	4th mode	5th mode
2	2922.86	6051.88	6393.08	10211.84	11275.11
4	5590.86	11883.54	12349.07	20052.83	21802.28
6	8166.61	17594.61	18105.40	29689.50	31902.52
8	10685.69	23176.16	23804.12	39185.09	41794.62
10	13166.40	28641.62	29471.20	48541.91	51509.83

To visualize the effect of variation of plate thickness on the free vibration behavior of composite plates in SSSS boundary condition, a graph is plotted below with the data of table 9. Each of the curves correspond to one of the modes.

Figure 4.10 Variation of frequency with plate thickness for a 15°skew laminate having no cut-out for SSSS condition. First five modes shown.

Table 10: Natural frequencies of 15°skew plates under CCCC boundary condition without cut out for various plate thicknesses

Mode→ Thickness (mm) ↓	1st mode	2nd mode	3rd mode	4th mode	5th mode
2	3875.96	7449.50	8118.06	12251.33	12701.82
4	7740.37	14866.85	16195.39	24416.59	25329.62
6	11582.39	22222.24	24194.01	36417.62	37815.07
8	15392.06	29488.81	32079.55	48186.26	50097.28
10	19160.37	36642.85	39821.60	59665.07	62123.60

To visualize the effect of variation of plate thickness on the free vibration behavior of composite plates in CCCC boundary condition, a graph is plotted below with the data of table 10. Each of the curves correspond to one of the modes.

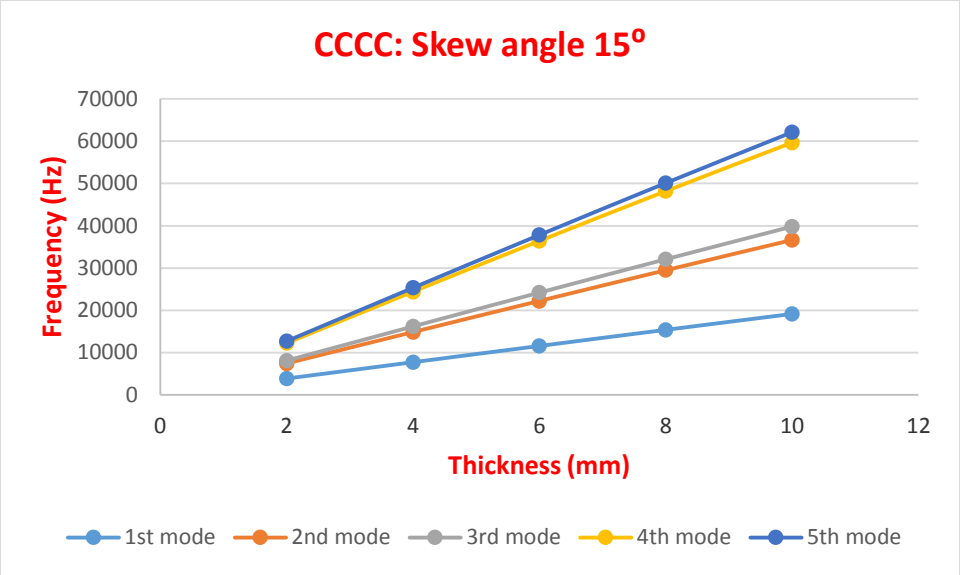

Figure 4.11 Variation of frequency with plate thickness for a 15° skew laminate having no cut-out for CCCC condition. First five modes shown.

To visualize the effect of variation of plate thickness on the free vibration behavior of composite plates in CCCC and SSSS boundary conditions, two graphs are plotted below with the data of tables 9 and 10. Each of the curves correspond to one of the boundary conditions.

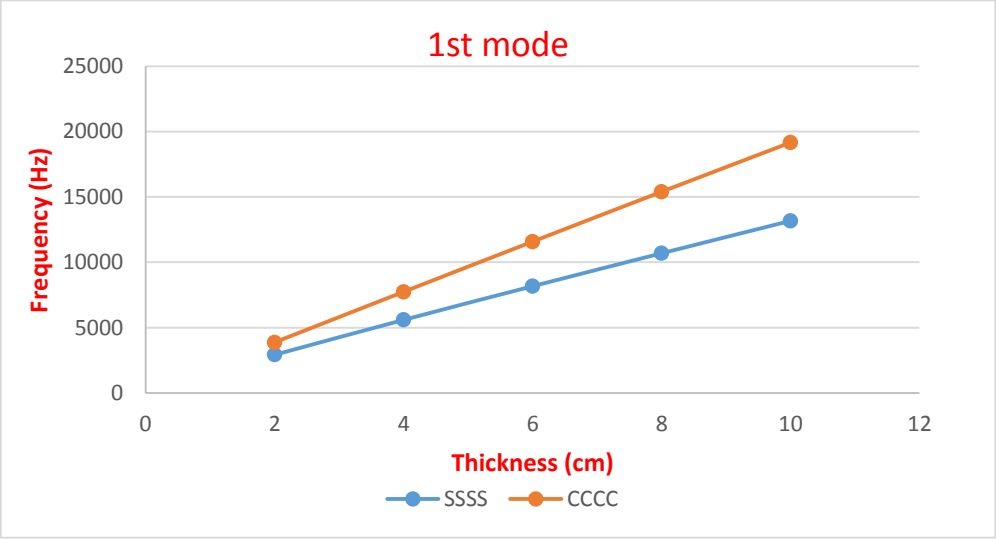

Figure 4.12 Variation of frequency with plate thickness for a 15° skew laminate having no cut-out for SSSS and CCCC conditions. First mode only is shown.

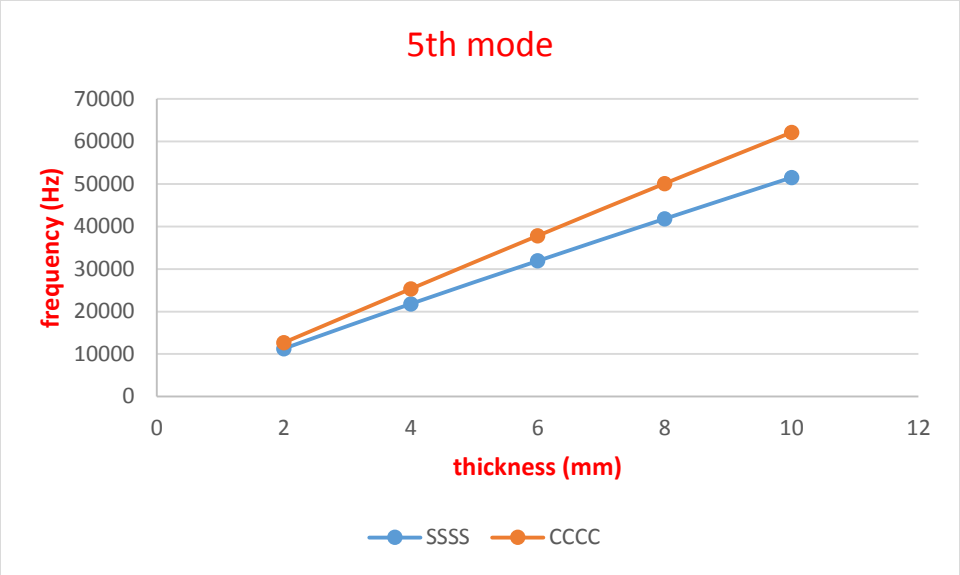

Figure 4.13 Variation of frequency with plate thickness for a 15^o skew laminate having no cut-out for SSSS and CCCC conditions. Fifth mode only is shown.

Observations from the above tables and figures:

1. In both SSSS and CCCC cases there is a continuous increase in value of frequency with increase in thickness. The rate of increase of frequency with thickness between any two thickness values is almost equal. Thus curves appear almost straight throughout.
2. In both SSSS and CCCC conditions the second mode and third mode frequencies are close in value to one another in all modes. Further, in both SSSS and CCCC conditions the fourth mode and fifth mode frequencies are quite close in value to one another in all modes. But with increase in laminate thickness, they become increasingly distinct.
3. For the fundamental mode, the values obtained for CCCC condition are always larger than those for SSSS condition. Moreover with increasing thickness the difference in frequency between CCCC and SSSS increases.
4. Other modes show similar behavior as well. But this trend decreases with increasing mode number. For fifth mode, the difference of values in frequency between CCCC and SSSS conditions is small through all thickness values.

4.3.4 Case study 4: Effect of variation due to cut out ratio

Four sizes of square cutouts, namely 0, 0.2, 0.4 and 0.6 are considered in order to examine the effect of cut-out size on the natural frequency of the laminate. Only centrally placed square cut outs without any delamination are considered in every case. Two studies are presented here in this regard, the first being for a skew angle of 0^o and the other for a skew angle of 15^o. The properties of the laminate, No. of layers, lay up sequence and dimensions of the plate are same as given in 4.3.

STUDY A: for skew angle 0^o

We vary the central cut out ratio (0, 0.2, 0.4 and 0.6) but keep the skew angle at 0^o throughout. The natural frequencies obtained thereby under SSSS condition are presented in table 11 below while those under CCCC condition are presented in table 12.

Table 11: Natural frequencies of SSSS square plates for various cut out ratios

Mode→ cut out ratio↓	1st	2nd	3rd	4th	5th
0	12049.67	24622.83	30439.10	41782.92	50352.17
0.2	11722.37	24024.14	28348.74	40844.80	49712.52
0.4	13255.44	22644.22	23185.00	39816.64	41559.82
0.6	18681.60	25211.09	26175.74	37457.19	45105.08

To visualize the effect of various cutout sizes on the free vibration behavior of composite plates two graphs are plotted with the data of table 11.

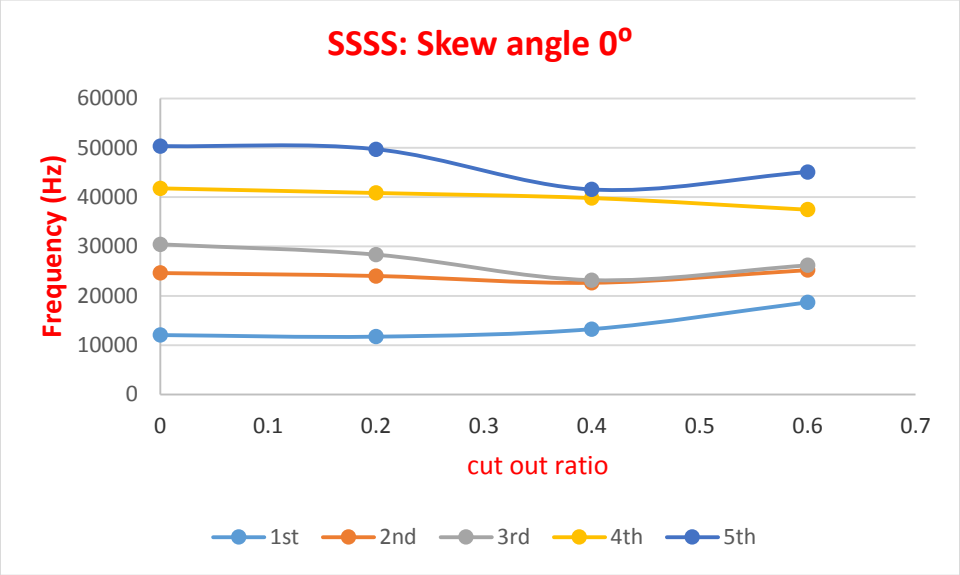

Figure 4.14 Variation of frequency with central cut out ratio for a square laminate for SSSS condition. First five modes are shown.

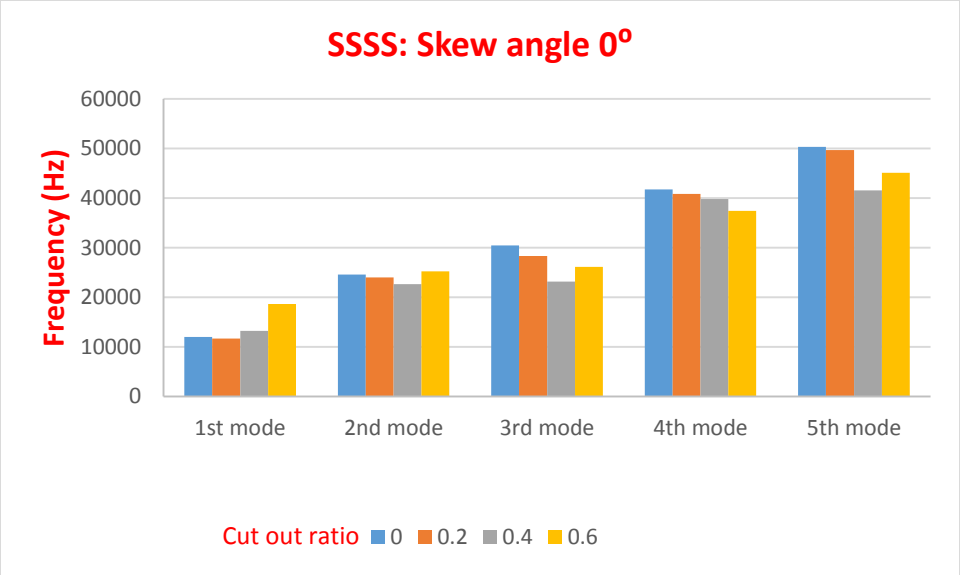

Figure 4.15 Variation of frequency with central cut out ratio for a square laminate for SSSS condition. First five modes are shown.

Now we do a similar study with CCCC case with same material properties and plate dimensions.

Table 12: Natural frequencies of CCCC square plates for various cut out ratios

Mode→ cut out ratio↓	1st	2nd	3rd	4th	5th
0	19132.62	34908.75	41132.46	54459.57	64571.58
0.2	19214.09	33690.00	37275.21	52877.31	63202.69
0.4	25438.89	33295.00	33986.88	51383.64	51476.71
0.6	47709.71	50982.08	52409.85	59370.16	67576.47

To visualize the effect of various cutout sizes on the free vibration behavior of composite plates two graphs are plotted with the data of table 12.

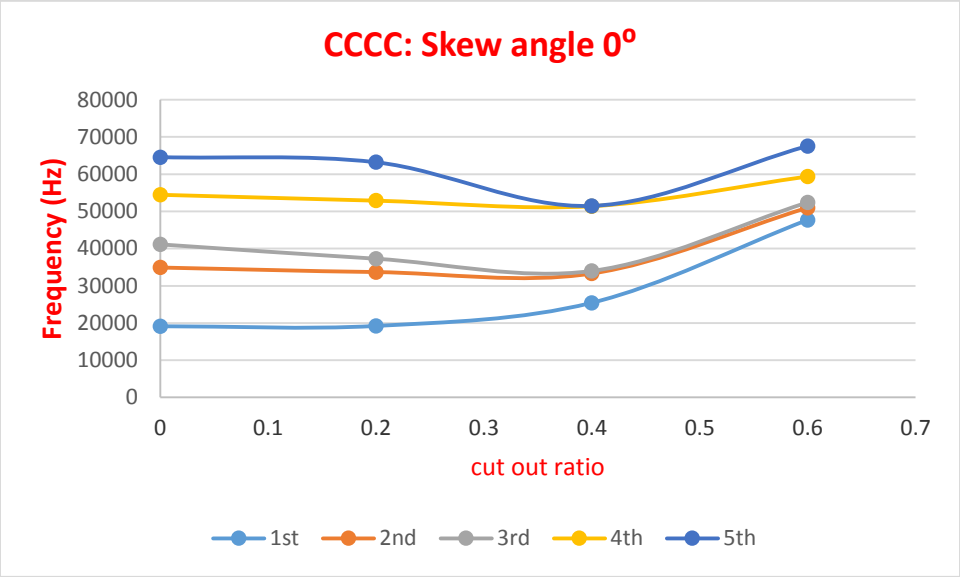

Figure 4.16 Variation of frequency with central cut out ratio for a square laminate for CCCC condition. First five modes are shown.

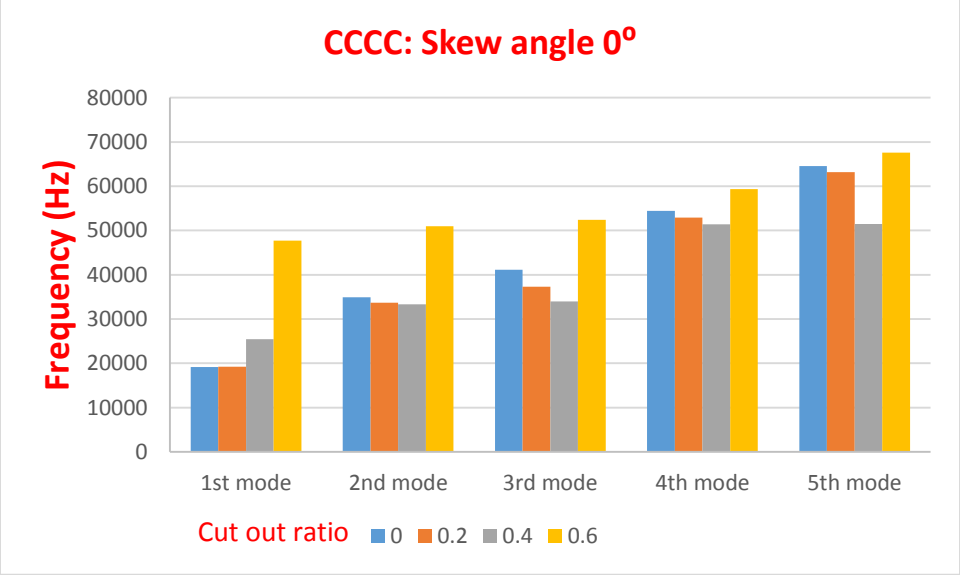

Figure 4.17 Variation of frequency with central cut out ratio for a square laminate for CCCC condition. First five modes are shown.

Observations from the above tables and figures:

1. The values of frequency for the 2nd and 3rd modes for higher values of central cut out size (like 0.4 and 0.6) are very close and the curves of these two modes are very similar in nature in both SSSS and CCCC cases.
2. In both SSSS and CCCC cases the fundamental frequency increases more or less as cut out ratio increases from 0 to 0.6 through 0.2 and 0.4.

3. The second and third modes show gentle decrease in frequency as cut out ratio increases from 0 to 0.2 and then to 0.4 in both SSSS and CCCC cases.
4. As cut out ratio increases from 0.4 to 0.6 in both SSSS and CCCC cases, the second and third modes show increase in frequency, percentage increase being more in CCCC case.
5. Values of frequency in a CCCC case is always more than the corresponding SSSS case.
6. Values of frequency for 0.6 cut out ratio in CCCC case is markedly more than in corresponding SSSS case for all modes. For example, fundamental frequency value for 0.6 cut out ratio is 60.84% more in CCCC case than in SSSS case. Similarly fifth mode frequency value for 0.6 cut out ratio is 33.25% more in CCCC case than in SSSS case.

STUDY B: for skew angle 15^o

Now, we vary the central cut out ratio (0, 0.2, 0.4 and 0.6) but keep the skew angle at 15^o throughout. The natural frequencies obtained thereby under SSSS condition are presented in table 13 below while those under CCCC condition are presented in table 14.

Table 13: Natural frequencies of SSSS 15^o skew plates for various cut out ratios

Mode → cut out ratio ↓	1st	2nd	3rd	4th	5th
0	13166.40	28641.62	29471.20	48541.91	51509.83
0.2	12962.09	27557.31	28118.71	46326.06	51374.48
0.4	15142.87	24333.09	25574.67	43051.46	44253.70
0.6	22389.37	27154.53	31546.27	41562.46	48677.07

To visualize the effect of various cutout sizes on the free vibration behavior of composite plates two graphs are plotted with the data of table 13.

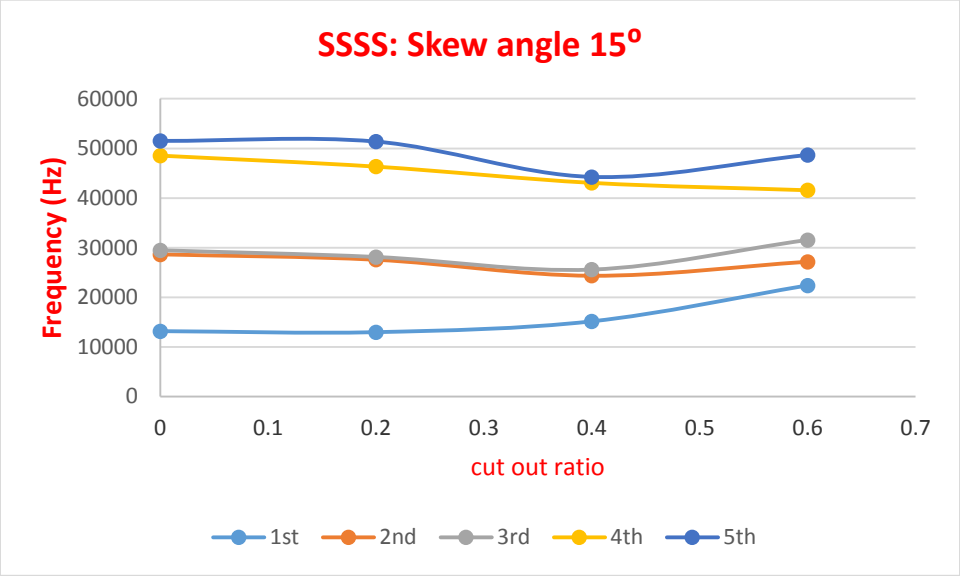

Figure 4.18 Variation of frequency with central cut out ratio for a 15^o skew laminate for SSSS condition. First five modes are shown.

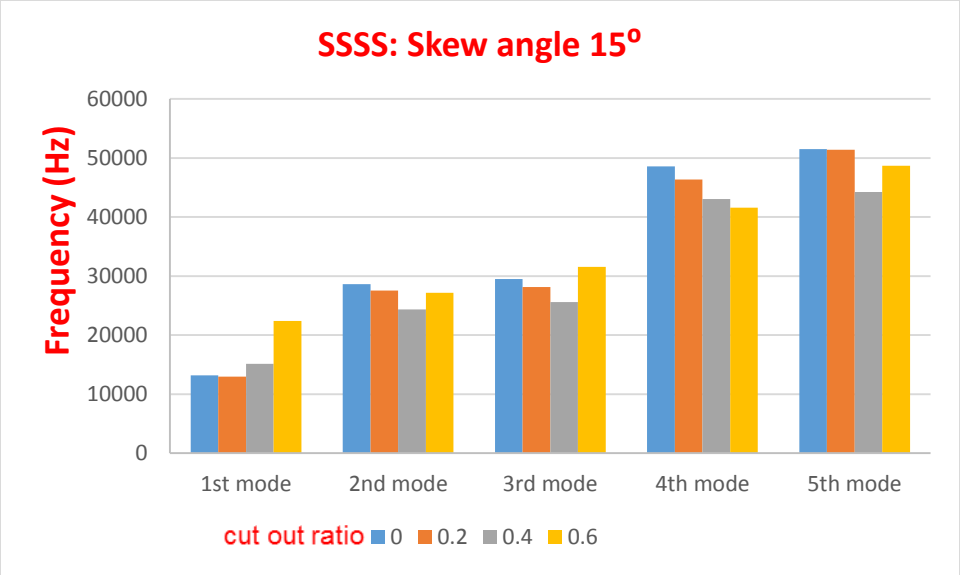

Figure 4.19 Variation of frequency with central cut out ratio for a 15° skew laminate for SSSS condition. First five modes are shown.

Table 147: Natural frequencies of CCCC 15° skew plates for various cut out ratios

Mode → cut out ratio ↓	1st	2nd	3rd	4th	5th
0	19160.37	36642.85	39821.60	59665.07	62123.60
0.2	19306.25	34840.17	37256.67	56484.81	62117.99
0.4	25498.42	33432.32	35117.63	52869.51	53302.04
0.6	47171.45	49702.62	54110.69	60746.68	68647.24

To visualize the effect of various cutout sizes on the free vibration behavior of composite plates, two graphs are plotted with the data of table 14.

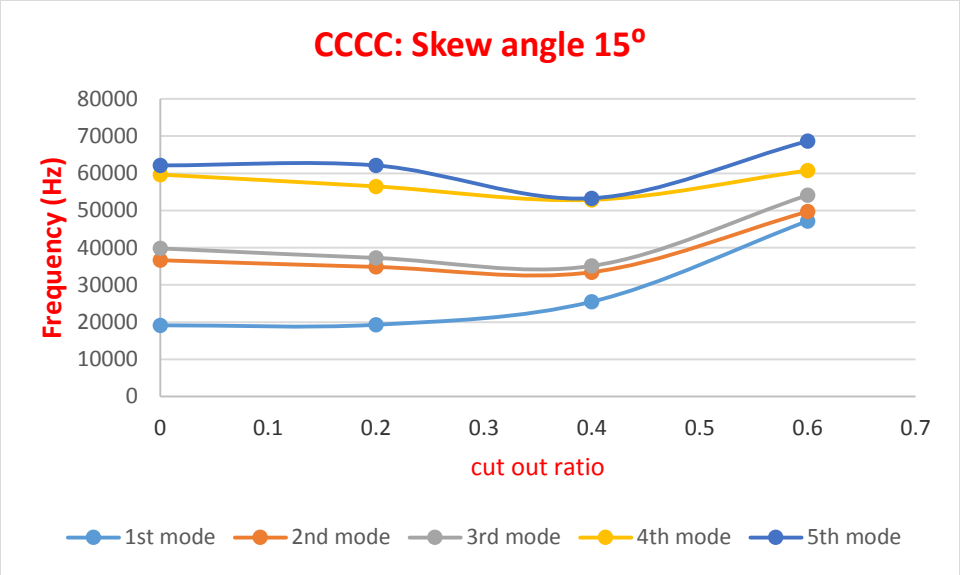

Figure 4.20 Variation of frequency with central cut out ratio for a 15° skew laminate for CCCC condition. First five modes are shown.

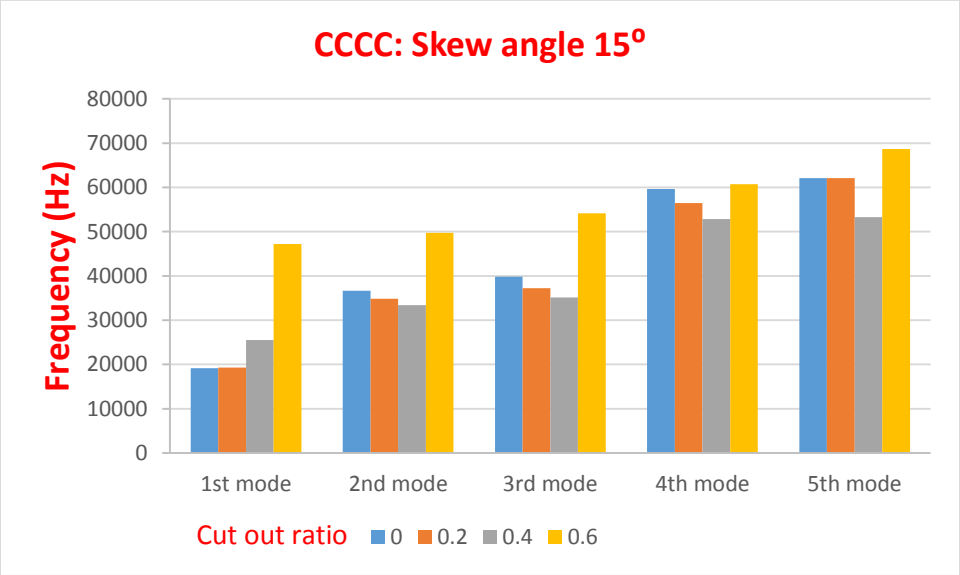

Figure 4.21 Variation of frequency with central cut out ratio for a 15° skew laminate for CCCC condition. First five modes are shown.

Observations from the above tables and figures:

1. The values of frequency for any value of central cut out size for the 2nd and 3rd modes are quite close and the curves of these two modes are very similar in nature in both SSSS and CCCC cases.
2. The values of frequency for any value of central cut out size for the 4th and 5th modes are somewhat close but even more noticeable is the fact that their curves are very similar in nature throughout in both SSSS and CCCC cases.
3. In both SSSS and CCCC cases the fundamental frequency increases more or less continuously as cut out ratio increases from 0 to 0.6 through 0.2 and 0.4.

4. The second and third modes show gentle decrease in frequency as cut out ratio increases from 0 to 0.2 and then gently increases to 0.4 in both SSSS and CCCC cases.
5. The fourth and fifth modes show gentle decrease in frequency as cut out ratio increases from 0 to 0.2 and then show further decrease in frequency as cut out ratio increases from 0.2 to 0.4 in both SSSS and CCCC cases.
6. As cut out ratio increases from 0.4 to 0.6 in both SSSS and CCCC cases, the second and third modes show increase in frequency, percentage increase being more in CCCC case.
7. As cut out ratio increases from 0.4 to 0.6 in both CCCC and SSSS cases a steep increase in frequency is observed (with the exception of fourth mode in SSSS).
8. Values of frequency in a CCCC case is always more than the corresponding SSSS case.
9. Values of frequency for 0.6 cut out ratio in CCCC case is markedly more than in corresponding SSSS case for all modes. For example, fundamental frequency value for 0.6 cut out ratio is 52.54% more in CCCC case than in SSSS case. Similarly fifth mode frequency value for 0.6 cut out ratio is 29.09% more in CCCC case than in SSSS case.

4.3.5 Case study 5: Effect of variation due to skew angle (cut out ratio 0.4)

The skew angle of the plate is now varied keeping a central cut out of fixed size i.e. of 0.4 cut out ratio in every case. Five skew angles, namely 0^o, 15^o, 30^o, 15^o and 60^o are considered in order to examine the effect of skew angle variation on the natural frequency of the laminate. Only a centrally placed square cut out of 0.4 cut out ratio without any delamination is considered in every case. The properties of the laminate, No. of layers, lay up sequence and dimensions of the plate are same as given in 4.3.

The natural frequencies for the first five modes obtained pertaining to SSSS condition are presented in table 15 while those pertaining to CCCC condition are presented in table 16.

Table 15: Natural frequencies of SSSS skew plates for various skew angles with cut out ratio of 0.4

Mode → Skew angle (°) ↓	1st	2nd	3rd	4th	5th
0	13255.44	22644.22	23185.00	39816.64	41559.82
15	15142.87	24333.09	25574.67	43051.46	44253.70
30	18565.84	26681.00	30538.50	47829.06	50199.21
45	24231.91	31835.98	38416.57	57503.21	59916.38
60	44170.77	48059.72	69319.27	87245.16	90163.65

To visualize the effect of variation of skew angle on the free vibration behavior of composite plates, a graph is plotted with the data of table 15.

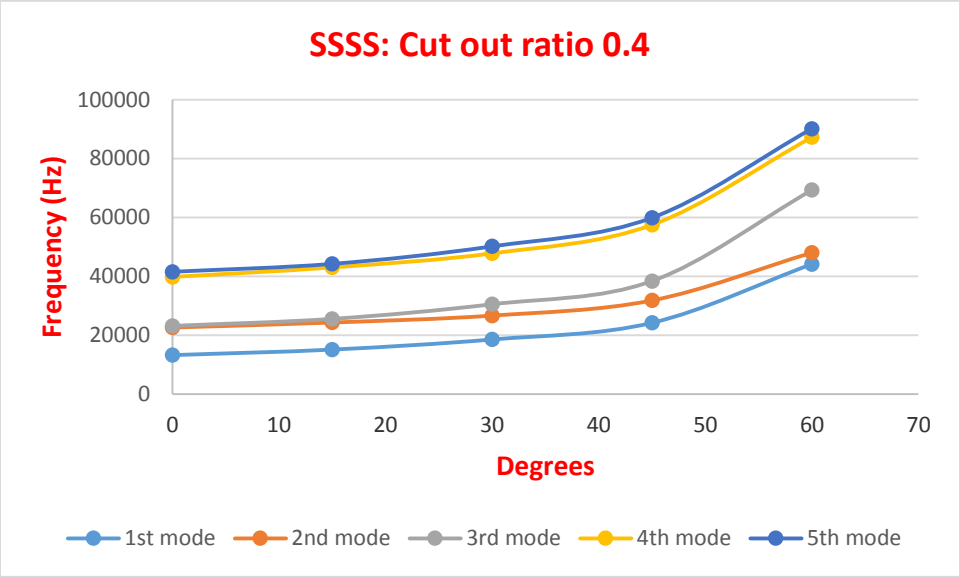

Figure 4.22 Variation of frequency with skew angle at a central cut out ratio of 0.4 for a laminate for SSSS condition. First five modes are shown.

Table 16: Natural frequencies of CCCC skew plates for various skew angles with cut out ratio of 0.4

Mode → Skew angle (°) ↓	1st	2nd	3rd	4th	5th
0	25438.89	33295.00	33986.88	51383.64	51476.71
15	25498.42	33432.32	35117.63	52869.51	53302.04
30	29929.86	37822.06	39953.56	58826.93	59647.53
45	41903.13	49053.42	53016.68	72613.35	74483.03
60	76075.10	81222.95	90967.71	107436.93	116044.54

To visualize the effect of variation of skew angle on the free vibration behavior of composite plates in CCCC boundary condition, a graph is plotted below with the data of table 16. Each of the curves correspond to one of the modes.

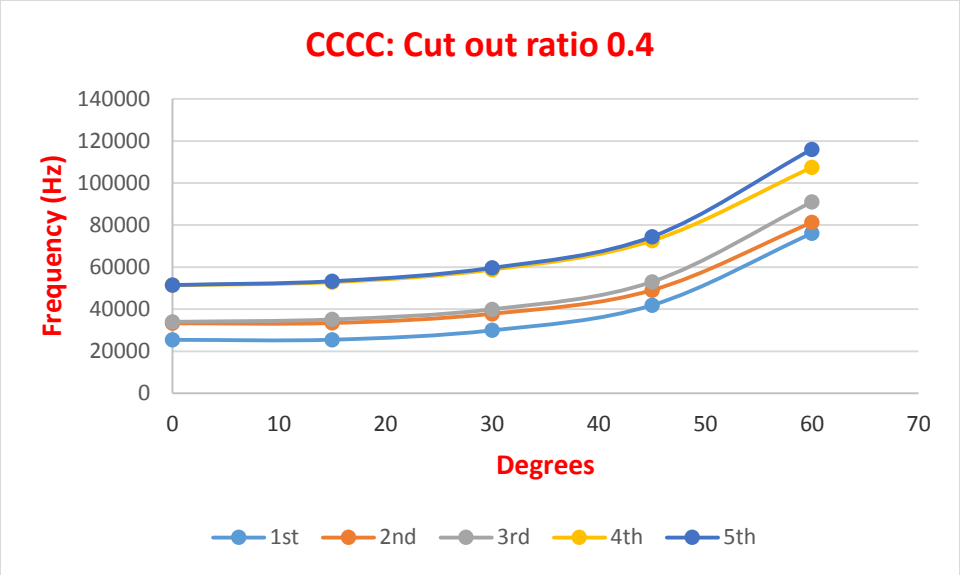

Figure 4.23 Variation of frequency with skew angle at a central cut out ratio of 0.4 for a laminate for CCCC condition. First five modes are shown.

To visualize the effect of variation of skew angle on the free vibration behavior of composite plates in SSSS and CCCC boundary conditions, a graph is plotted below with the data of table 15 and 16. Each of the curves represent a boundary condition.

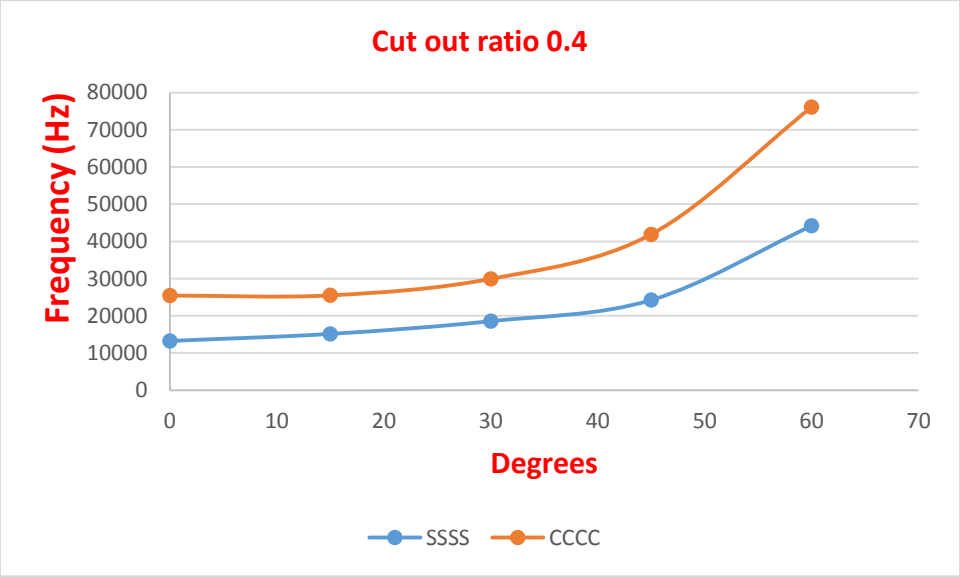

Figure 4.24 Variation of frequency with skew angle at a central cut out ratio of 0.4 for a laminate for SSSS and CCCC conditions. First mode only is shown.

Observations from the above tables and figures:

1. In both SSSS and CCCC cases there is a continuous increase in value of frequency with increase in skew angle but for smaller values of skew angle, say up to 30^{o}, the percentage increase of frequency is not much whereas for higher values of skew angles like 45^{o} or 60^{o} the percentage

increase of frequency is great. To illustrate this point let us take the case of increase of skew angle from 0^o to 30^o in CCCC condition where the corresponding increase of frequency is 15.00% in first mode but with increase in skew angle from 45^o to 60^o, the corresponding increase of frequency is 44.92% for the same mode and boundary condition.

2. In both SSSS and CCCC cases the nature of curves is similar in general i.e. percentage increase of frequency between two consecutive values of skew angle is quite similar though this not strictly true for the skew angles 45 and 60 degrees..
3. Though the nature of the curves for fundamental frequency for both SSSS and CCCC are very similar, the frequencies are always greater for the CCCC case.
4. The values of frequency for any value of skew angle for the 2nd and 3rd modes are very close and the curves of these two modes are very similar in nature in both SSSS and CCCC cases. Though these two curves become distinct with increase skew angle and it is more so in SSSS case.
5. The values of frequency for any value of skew angle for the 4th and 5th modes are very close throughout in both SSSS and CCCC cases.

5 CONCLUSION

1. There is a continuous increase in value of frequency with increase in skew angle but for smaller values of skew angle, say up to 30^o, the percentage increase of frequency is not much whereas for higher values of skew angles like 45^o or 60^o the percentage increase of frequency is greater.
2. For every mode, the highest frequency is always from the CCCC condition and the lowest frequency is from the SSSS condition. One may infer that increasing the degree of constraints at the boundary has the effect of increasing the stiffness of the plate.
3. There is a continuous increase in value of frequency with increase in thickness. The rate of increase of frequency with thickness between any two thickness values is almost equal. Thus curves appear almost straight throughout.
4. The fundamental frequency increases more or less as cut out ratio increases from 0 to 0.6 through 0.2 and 0.4.
5. In all cases of plate structures with central cut-out being symmetric, the second and third mode frequencies are quite close in general.
6. The values of frequency in general for the 4th and 5th modes are somewhat close but even more noticeable is the fact that their curves are very similar in nature throughout.

6 FUTURE SCOPE OF STUDY

The finite element technique was adopted in the present study to carry out the frequency analysis of multilayered laminated composites with centrally located square and circular cutouts. The formulation developed here is general in nature and employs a nine noded Lagrangian element for finite element formulation. The possible extensions to future study can be:

1. Parametric studies varying the aspect ratio of the plate, shape of cutout (circular cutout and rectangular cutout), location of cutout and number of layers of plate need to be studied.
2. These parametric studies can be conducted with other materials like glass/epoxy, etc.
3. The present formulation is based on first order shear deformation theory. It can be modified to take higher order shear deformation theory into account.
4. This study may be extended to stiffened plates with cutout.

5. Both experimental and numerical analysis and convergence of numerical and experimental data of plates with delamination around cutout can be studied for advanced research work.
6. Different types of elements can be used to carry out the finite element analysis and the results can be analysed for accuracy of results.
7. Stability can be another scope of study.
8. Study of forced vibration behaviour may be performed.
9. Hygrothermal behaviour may be studied.

7 REFERRENCES

1. Liu DS and Li XY. An overall view of laminate theories based on displacement hypothesis. J Compos Mater 1996; 30:1539–61.
2. Kant T and Swaminathan K. Estimation of transverse/interlaminar stresses in laminated composites –a selective review and survey of current developments. Composite Structure 2000; 49:65–75.
3. Jones RM. Bending, Buckling and Vibration of Laminated plates, Chapter5, Mechanics of Composite Materials, McGraw-Hill Kogakusha Ltd. Tokyo, 1975.
4. Kirchhoff G. 1850, Über das Gleichgewicht und die Bewegungeiner Elastischen Scheibe, J. Angew. Math., 40, 51.
5. Mindlin RD. Influence of Rotary Inertia and Shear on the Flexural Motions of IsotropicElastic Plates, Journal of Applied Mechanics, 1951; Transactions of the ASME, 18, 31-38.
6. Stavsky Y. On the Theory of Symmetrically Heterogeneous Plates Having the Same Thickness Variation of the Elastic Moduli, “Topics in Applied Mechanics”, 1965; Eds.Abir, D. F. Ollendorff and M. Reiner, American Elsevier
7. Yang PC, Norris CH and Stavsky Y. Elastic Wave Propagation in Heterogeneous Plates, International Journal of Solids and Structures, 1966; 2, 665-684.
8. Seide, P., Small Elastic Deformations of Thin Shells, Noordhoff, The Netherlands, 1975.
9. Srinivas, S, and Rao, A.K., 'Bending, vibration and buckling of simply supported thick orthotropic rectangular plates and laminates', International Journal of Solids and Structures 6, 1970, 1463-1481.
10. Srinivas, S., Joga Rao, C. V., and Rao, A. K., 'An exact analysis for vibration of simply-supported and laminated thick rectangular plates', Journal of Sound and Vibration 12, 1970, 187-199.
11. Pagano, N. J., 'Exact solutions for rectangular bidirectional composites and sandwich plates', Journal of Composite Materials 4, 1970, 20-34.
12. Pagano, N. J. and Hatfield, S. J., ‘Elastic behavior of multilayer bidirectional composites', AIAA Journal 10, 1972, 931-933.
13. Adams, R. D. and Bacon, D. G. C., 'Measurement of the flexural damping capacity and dynamic Young's modulus of metals and reinforced plastics', Journal of Physics D: Applied Physics 6, 1973, 27-41.
14. Reissner E. On the Theory of Bending of Elastic Plates, Journal of Mathematical Physics, 1944; 23, 184.
15. Reissner, E., 'The effect of transverse shear deformation on the bending of elastic plates', Journal of Applied Mechanics 12(1), 1945, A-69 to A-77.
16. Reissner, E., 'On bending of elastic plates', Quarterly of Applied Mathematics 5, 1947, 55-68.

17. Basset, A. B., 'On the extension and flexure of cylindrical and spherical thin elastic shells', Philosophical Transactions of the Royal Society of London Ser. A, 181(6), 1890, 433-480.
18. Hildebrand, F. B., Reissner, E., and Thomas, G. B., 'Note on the foundations of the theory of small displacements of orthotropic shells', NACA Technical Note No. 1833, March 1949.
19. Hencky, H., 'Uber die Berucksichtigung der Schubverzerrung in ebenen Platten', Ingenieur Archly 16, 1947, 72-76.
20. Whitney, J.M., The Effect of Transverse Shear Deformation on the Bending of Laminated Plates, J. Appl. Mech., Vol. 36, 534-547. 1969.
21. Srinivas S, Joga Rao CV and Rao AK. An Exact Analysis of Vibration of Simply supported Homogeneous Laminated Thick Rectangular Plates, Journal of Sound and Vibration, 1970; 12, 187-199.
22. Sun, C.T. and Whitney, J.M., Theories for the Dynamic Response of Laminated Plates, AIAA J., Vol. 11, 178-183, 1973.
23. Mau ST, Pjan THH and Tong P. Vibration Analysis of Laminated Plates and Shells by a Hybrid Stress Element, AIAA Journal, 1973; 11, 1450-1452.
24. Hinton E. A Note on a Thick Finite Strip Method for the Free Vibration of Laminated Plates, Earthquake Engineering and Structural Dynamics, 1976; 4, 511—514.
25. Hinton E. A Note on a Finite Element Method for the Free Vibrations of Laminated Plates, Earthquake Engineering and Structural Dynamics, 1976; 4, 515-516.
26. Bert CW and Chen TL. Effect of Shear Deformation on Vibration of Antisymmetric Angle-Ply Laminated Rectangular Plates, Journal of Solids and Structures, 1978; 14, 465-473.
27. Yoshihiro Narita. Doctoral dissertation on “FREE VIBRATION OF ELASTIC PLATES WITH VARIOUS SHAPES AND BOUNDARY CONDITIONS” presented to the Graduate School of Engineering, Hokkaido University in December, 1979.
28. Reddy JN. Free Vibration of Anti-symmetric Angle-ply Laminated Plates Including Transverse Shear Deformation by the Finite Element Method, Journal of Sound and Vibration, 1979; 66, 565-576
29. Lo, K.H, Christensen, R.M. and Wu, E.M., A High-Order Theory of Plate Deformation, Part 2: Laminated Plates, J. Appl. Mech., Vol. 44, 669-676, 1977
30. Seide, P., An Approximate Theory for the Bending of Laminated Plates, MECAHNICS TODAY, N. Nasser (ed.), Vol. 5, 451-466, 1980.
31. Putcha NS and Reddy JN. Stability and Vibration Analysis of Laminated Plates by using a Mixed Element Based on Refined Plate Theory, Journal of Sound and Vibration, 1986; 104, 285-300.
32. Craig TJ and Dawe DJ. Flexural Vibration of Symmetrically Laminated Composite Rectangular Plates Including Transverse Shear Effects, International Journal of Solids and Structures, 1986; 22, 155-169.
33. R. S. Sandhu, W. E. Wolfe, S. J. Hong, and H. S. Chohan. Final Report for Period July 1985 -August 1990, Department of Civil Engineering, The Ohio State University for National Technical Information Service
34. Fares M.E. and Zenkour A.M. Buckling and free vibration of non-homogeneous composite cross-ply laminated plates with various plate theories, Composite Structures, April 1999; Volume 44, Issue 4, Pages 279-287.
35. Y.Y. Wang, K.Y. Lam, G.R. Liu. A strip element method for the transient analysis of symmetric laminated plates, International Journal of Solids and Structures 38 (2001), 241-259
36. Reddy, J.N., 'A review of the literature on finite-element modeling of laminated composite plates', Shock and Vibration Digest 17, 1985, 3-8.
37. Librescu, L., Khdeir, A. A., and Reddy, J. N., 'A comprehensive analysis of the state of stress of elastic anisotropic flat plates using refined theories', Acta Mechanica 70, 1987, 57-81

38. Librescu, L. and Khdeir, A. A., 'Analysis of symmetric cross-ply laminated elastic plates using a higher-order theory: part I- stress and displacement', Composite Structures 9, 1988, 189-213.
39. Khdeir, A. A. and Librescu, L., 'Analysis of symmetric cross-ply laminated elastic plates using a higher-order theory: part II- buckling and free vibration', Composite Structures 9,1988, 259-277
40. Paramasivam P. Free vibration of square plates with square openings. J Sound Vibration 1973; 30: 173–8.
41. Aksu G and Ali R. Determination of dynamic characteristics of rectangular plates with cutouts using a finite difference formulation. J Sound Vibration 1976; 44:147–58.
42. Rajamani A and Prabhakaran R. Dynamic response of composite plates with cutouts. Part I: Simply-supported plates. J Sound Vibration 1977; 54: 549–64.
43. Rajamani A and Prabhakaran R. Dynamic response of composite plates with cutouts. Part II: Clamped–clamped plates. J Sound Vibration 1977; 54: 565–76.
44. Ali R and Atwal SJ. Prediction of natural frequencies of vibration of rectangular plates with rectangular cutouts. Comput Structures 1980; 12: 819–23.
45. Reddy JN. Large amplitude flexural vibration of layered composite plates with cutouts. J Sound Vibration 1982; 83:1–10.
46. Lee HP, Lim SP and Chow ST. Free vibration of composite rectangular plates with rectangular cutouts. Compos Structures 1987; 8: 63–81.
47. Chang CN and Chiang FK. Vibration analysis of a thick plate with an interior cutouts by a finite element methods. J Sound Vibration 1988; 125: 477–86.
48. Nagaya K. Simplified method for solving problems of vibrating plates of doubly connected arbitrary shape. Part I: Derivation of frequency equation. J Sound Vibration 1981; 74: 543–51.
49. Nagaya K. Simplified method for solving problems of vibrating plates of doubly connected arbitrary shape. Part II: Applications and experiments. J Sound Vibration 1981; 74: 553–64.
50. Mundkar G, Bhat RB and Neriya S. Vibration of plates with cutouts using boundary characteristic orthogonal polynomial functions in the Rayleigh–Ritz method. J Sound Vibration 1994; 176: 136–44.
51. Sabir AB and Davies GT. Natural frequencies of plates with square holes when subjected to in-plane uniaxial, biaxial or shear loading. Thin-Walled Structures 1997; 29: 312–35.
52. Rossi RE. Transverse vibrations of thin, orthotropic rectangular plates with rectangular cutouts with fixed boundaries. J Sound Vibration 1999; 221:733–6.
53. Chen CC, Kitiporanchai S, Lim CW and Liew KM. Free vibration of symmetrically laminated thick perforated plates. J Sound Vibration 2000; 230:111–32.
54. Kumar A and Shrivastava RP. Free vibration of square laminates with delamination around a central cutout using HSDT. Composite Structures 70 (2005) 317–333.
55. Hota SS and Padhi P. Vibration of plates with arbitrary shapes of cutouts. Journal of Sound and Vibration 302 (2007) 1030–1036.
56. Dash S, Asha AV and Sahu SK. Stability of laminated composite curved panels with cutout using finite element method. Presented on International Conference in Theoretical, Applied Computational and experimental Mechanics (ICTACEM 2004) during December 28-31, 2004 at IIT, Kharagpur.
57. Sivakumar K, Iyenger NGR and Deb K. Free vibration of laminated composite plates with cutout. Journal of Sound and Vibration (1999) 221(3), 443-470.
58. Iyenger NGR and Bhavani Prasad A. Optimal design of composite laminates with and without cutout undergoing free vibration. The IES Journal Part A: Civil & Structural Engineering, Vol. 3, No. 3, August 2010, 161–167.

59. Laura PAA, Verniere De Irassar P and Ercoli L. Fundamental frequency of a rectangular plate with a free, straight corner cutout. Journal of Sound and Vibration (1981) 78(4), 489-493.
60. Turvey GJ, Mulcahy N and Widden MB. Experimental and computed natural frequencies of square pultruded GRP plates: effects of anisotropy, hole size ratio and edge support conditions. Composite Structures 50 (2000) 391-403.
61. Khdeir AA and Reddy JN. Free vibrations of laminated composite plates using second order shear deformation theory. Computers and Structures 71 (1999) 617-626.
62. Lee HP, Lim SP and Chow ST. Free Vibration of Composite Rectangular Plates with Rectangular Cutouts. Composite Structures 8 (1987) 63-81.
63. Rezaeepazhand J and Jafari N. Stress analysis of perforated composite plates, Composite Structures 71 (2005) 463–468.
64. Beslin O and Guyader JL. The use of an ‘‘ectoplasm’’ to predict free vibrations of plates with cut-outs, Journal of Sound and Vibrations 191 (5) (1996) 935–954.
65. Huang M and Sakiyama T, Free vibration analysis of rectangular plates with variously shaped holes, Journal of Sound and Vibration 226 (4) (1999) 769–786.
66. Reddy JN 1984, A simple higher order theory for laminated composite plates. Transactions of the American Society of Mechanical Engineers, Journal of Applied Mechanics 51, 745-752.
67. A. Houmat, Nonlinear free vibration analysis of variable stiffness symmetric skew laminates, European Journal of Mechanics A/Solids 50 (2015) 70-75.
68. P. Malekzadeh, Differential quadrature large amplitude free vibration analysis of laminated skew plates based on FSDT, Composite Structures 83 (2008) 189–200.
69. M.K. Singha, Rupesh Daripa, Nonlinear vibration of symmetrically laminated composite skew plates by finite element method, International Journal of Non-Linear Mechanics 42 (2007) 1144–1152.
70. Maloy K. Singha, M. Ganapathi, Large amplitude free flexural vibrations of laminated composite skew plates, International Journal of Non-Linear Mechanics 39 (2004) 1709–1720.
71. S. Wang, Free vibration analysis of skew fibre-reinforced composite laminates based on first-order shear deformation plate theory, Computers & Structures Vol. 63, No. 3, pp. 525-538, 1997.
72. Sang-Youl Lee, Finite element dynamic stability analysis of laminated composite skew plates containing cutouts based on HSDT, Composites Science and Technology 70 (2010) 1249–1257.
73. T. Park, S.-Y. Lee, G.Z. Voyiadjis, Finite element vibration analysis of composite skew laminates containing delaminations around quadrilateral cutouts, Composites: Part B 40 (2009) 225–236.